Impact Factor:						
	ISRA (India)	= **6.317**	**SIS** (USA)	= **0.912**	**ICV** (Poland)	= **6.630**
	ISI (Dubai, UAE)	= **1.582**	**РИНЦ** (Russia)	= **3.939**	**PIF** (India)	= **1.940**
	GIF (Australia)	= **0.564**	**ESJI** (KZ)	= **8.771**	**IBI** (India)	= **4.260**
	JIF	= **1.500**	**SJIF** (Morocco)	= **7.184**	**OAJI** (USA)	= **0.350**

SOI: 1.1/TAS DOI: 10.15863/TAS

International Scientific Journal

Theoretical & Applied Science

p-ISSN: 2308-4944 (print) **e-ISSN:** 2409-0085 (online)

Year: 2022 **Issue:** 05 **Volume:** 109

Published: 21.05.2022 **http://T-Science.org**

Issue **Article**

Denis Chemezov
Vladimir Industrial College
M.Sc.Eng., Corresponding Member of International Academy of Theoretical and Applied Sciences, Lecturer, Russian Federation
https://orcid.org/0000-0002-2747-552X
vic-science@yandex.ru

Anzhelika Bayakina
Vladimir Industrial College
Lecturer, Russian Federation

Daniil Zavrazhnov
Vladimir Industrial College
Student, Russian Federation

Elena Stepanova
Vladimir Industrial College
Lecturer, Russian Federation

Artyom Gorechnin
Vladimir Industrial College
Student, Russian Federation

Georgiy Karatun
Vladimir Industrial College
Student, Russian Federation

Aleksey Kuzin
Vladimir Industrial College
Student, Russian Federation

Nikolay Kornev
Vladimir Industrial College
Student, Russian Federation

REFERENCE DATA OF PRESSURE DISTRIBUTION ON THE SURFACES OF AIRFOILS HAVING THE NAMES BEGINNING WITH THE LETTER H (THE SECOND PART)

Abstract: *The results of the computer calculation of air flow around the airfoils having the names beginning with the letter H (continuation) are presented in the article. The contours of pressure distribution on the surfaces of the airfoils at the angles of attack of 0, 15 and -15 degrees in conditions of the subsonic airplane flight speed were obtained.*

Key words: *the airfoil, the angle of attack, pressure, the surface.*
Language: *English*

Citation: Chemezov, D., et al. (2022). Reference data of pressure distribution on the surfaces of airfoils having the names beginning with the letter H (the second part). *ISJ Theoretical & Applied Science, 05 (109)*, 529-586.
Soi: http://s-o-i.org/1.1/TAS-05-109-57 ***Doi***: https://dx.doi.org/10.15863/TAS.2022.05.109.57
Scopus ASCC: *1507.*

Introduction

Creating reference materials that determine the most accurate pressure distribution on the airfoils surfaces is an actual task of the airplane aerodynamics.

Materials and methods

The study of air flow around the airfoils was carried out in a two-dimensional formulation by means of the computer calculation in the *Comsol Multiphysics* program. The airfoils in the cross section were taken as objects of research [1-22]. In this work, the airfoils having the names beginning with the letter *H* were adopted. Air flow around the airfoils was carried out at the angles of attack (α) of 0, 15 and -15 degrees. Flight speed of the airplane in each case was subsonic. The airplane flight in the atmosphere was carried out under normal weather conditions. The geometric characteristics of the studied airfoils are presented in the Table 1. The geometric shapes of the airfoils in the cross section are presented in the Table 2.

Table 1. The geometric characteristics of the airfoils.

Airfoil name	Max. thickness	Max. camber	Leading edge radius	Trailing edge thickness
HN-464	8.35% at 31.6% of the chord	2.05% at 46.9% of the chord	0.5054%	0.0%
HN-465	8.35% at 31.6% of the chord	2.25% at 46.9% of the chord	0.5045%	0.0%
HN-785	7.85% at 31.6% of the chord	1.88% at 43.7% of the chord	0.4615%	0.0%
HN-785SR	7.85% at 31.6% of the chord	1.48% at 43.7% of the chord	0.4689%	0.0%
HN-801	8.5% at 31.6% of the chord	2.0% at 43.7% of the chord	0.5281%	0.0%
HN-805	7.85% at 31.6% of the chord	1.55% at 43.7% of the chord	0.4683%	0.0%
HN-808	10.32% at 31.6% of the chord	2.02% at 46.9% of the chord	0.7338%	0.0%
HN-832	11.35% at 28.7% of the chord	2.36% at 46.9% of the chord	0.8957%	0.0%
HN-832TA	11.55% at 28.7% of the chord	2.4% at 46.9% of the chord	0.9268%	0.0%
HN-951	10.85% at 31.6% of the chord	1.85% at 43.7% of the chord	0.8189%	0.0%
HN-956	13.14% at 31.6% of the chord	2.3% at 46.9% of the chord	1.0373%	0.0%
HN-961SA	10.15% at 28.7% of the chord	0.35% at 46.9% of the chord	0.8637%	0.0%
HN-971	10.85% at 28.7% of the chord	2.38% at 43.7% of the chord	0.8537%	0.0%
HN-972	10.25% at 28.7% of the chord	2.48% at 43.7% of the chord	0.7676%	0.0%
HN-973	8.33% at 31.6% of the chord	2.38% at 43.7% of the chord	0.5249%	0.0%
HN-974	12.32% at 31.6% of the chord	2.43% at 46.9% of the chord	0.8802%	0.0%
HN-975	12.32% at 31.6% of the chord	2.55% at 46.9% of the chord	0.8894%	0.0%
HN-975TA	12.55% at 31.6% of the chord	2.65% at 46.9% of the chord	0.9099%	0.0%
HN-976S	11.19% at 25.9% of the chord	0.0% at 0.0% of the chord	0.8307%	0.0%
HN-979	7.52% at 28.7% of the chord	2.14% at 46.9% of the chord	0.4512%	0.0%
HN979D	6.55% at 28.7% of the chord	1.75% at 46.9% of the chord	0.3764%	0.0%
HN-980	11.54% at 31.6% of the chord	1.74% at 46.9% of the chord	0.7783%	0.0%
HN-981	8.05% at 31.6% of the chord	1.88% at 46.9% of the chord	0.475%	0.0%
HN-989	8.04% at 28.7% of the chord	1.85% at 46.9% of the chord	0.4586%	0.0%
HN-990	7.85% at 31.6% of the chord	1.88% at 43.7% of the chord	0.4713%	0.0%
HN-997A	7.52% at 28.7% of the chord	2.52% at 46.9% of the chord	0.4495%	0.0%
HN-997B	7.52% at 28.7% of the chord	2.85% at 46.9% of the chord	0.4481%	0.0%
HN-998	6.87% at 28.7% of the chord	2.97% at 46.9% of the chord	0.387%	0.0%
HN-999	7.05% at 31.6% of the chord	3.03% at 46.9% of the chord	0.3908%	0.0%
HO1	9.99% at 47.3% of the chord	0.13% at 1.3% of the chord	2.4387%	1.65%
HO1U	7.0% at 47.3% of the chord	0.13% at 1.3% of the chord	2.4695%	1.156%
HO2	12.0% at 34.3% of the chord	4.38% at 42.9% of the chord	3.2328%	2.432%
HOBIE	8.49% at 25.0% of the chord	3.96% at 45.0% of the chord	1.5473%	0.0%
Hobie Hawk	8.49% at 25.0% of the chord	3.96% at 45.0% of the chord	0.4767%	0.0%
HOBIE-SM	8.57% at 25.0% of the chord	3.98% at 45.0% of the chord	0.7412%	0.0%
HOBIESMO1,DAT	8.57% at 25.0% of the chord	3.98% at 45.0% of the chord	0.7412%	0.0%
HORSTMANN AND QUAST HQ-300 GD(MOD 2)	16.58% at 37.1% of the chord	3.74% at 37.1% of the chord	1.2756%	0.3575%
Horten Standard 13%	13.0% at 30.0% of the chord	2.14% at 30.0% of the chord	1.2823%	0.0%
HQ 0-10	10.0% at 33.9% of the chord	0.0% at 0.0% of the chord	0.6487%	0.0%
HQ 0-7	7.0% at 33.9% of the chord	0.0% at 0.0% of the chord	0.4051%	0.0%
HQ 0-9	8.11% at 33.9% of the chord	0.0% at 0.0% of the chord	0.4787%	0.0%
HQ 1,0-10	9.96% at 35.0% of the chord	1.0% at 50.0% of the chord	0.5002%	0.0%
HQ 1,0-12	11.96% at 35.0% of the chord	1.0% at 50.0% of the chord	0.7389%	0.0%
HQ 1,0-8	7.97% at 35.0% of the chord	1.0% at 50.0% of the chord	0.3215%	0.0%

HQ 1,0-9	8.98% at 35.0% of the chord	1.0% at 50.0% of the chord	0.4044%	0.0%
HQ 1,5-10	9.96% at 35.0% of the chord	1.5% at 50.0% of the chord	0.5144%	0.0%
HQ 1,5-11	11.0% at 33.9% of the chord	1.5% at 50.0% of the chord	0.8289%	0.0%
HQ 1,5-12	11.96% at 35.0% of the chord	1.5% at 50.0% of the chord	0.7783%	0.0%
HQ 1,5-8	7.96% at 32.5% of the chord	1.49% at 50.0% of the chord	0.3262%	0.0%
HQ 1,5-8,5	8.56% at 35.0% of the chord	1.5% at 50.0% of the chord	0.3939%	0.0%
HQ 1,5-9	8.97% at 35.0% of the chord	1.5% at 50.0% of the chord	0.413%	0.0%
HQ 1,5-9 B	8.95% at 37.1% of the chord	1.5% at 50.0% of the chord	0.3622%	0.0%
HQ 2,0-10	9.97% at 35.0% of the chord	2.0% at 50.0% of the chord	0.5145%	0.0%
HQ 2,0-11	10.97% at 35.0% of the chord	2.0% at 45.0% of the chord	0.628%	0.0%
HQ 2,0-12	11.97% at 35.0% of the chord	1.99% at 50.0% of the chord	0.7652%	0.0%
HQ 2,0-13	12.96% at 35.0% of the chord	2.0% at 50.0% of the chord	0.8939%	0.0%
HQ 2,0-8	7.98% at 35.0% of the chord	1.99% at 50.0% of the chord	0.33%	0.0%
HQ 2,0-9	8.97% at 35.0% of the chord	1.99% at 50.0% of the chord	0.4164%	0.0%
HQ 2,1-9,5	9.49% at 35.0% of the chord	2.1% at 55.0% of the chord	0.6756%	0.001%
HQ 2,5-10	9.96% at 35.0% of the chord	2.5% at 50.0% of the chord	0.4372%	0.0%
HQ 2,5-11	11.0% at 33.9% of the chord	2.5% at 50.0% of the chord	0.7559%	0.0%
HQ 2,5-12	11.96% at 35.0% of the chord	2.5% at 50.0% of the chord	0.6646%	0.0%
HQ 2,5-14	13.95% at 35.0% of the chord	2.5% at 50.0% of the chord	0.8848%	0.0%
HQ 2,5-8	7.97% at 35.0% of the chord	2.5% at 50.0% of the chord	0.2831%	0.0%
HQ 2,5-9	8.97% at 35.0% of the chord	2.5% at 50.0% of the chord	0.3533%	0.0%
HQ 2,5-9 B	9.03% at 35.0% of the chord	2.53% at 55.0% of the chord	0.5932%	0.0%
HQ 2,5-9,0 smoothed by Eppler	9.03% at 35.0% of the chord	2.53% at 55.0% of the chord	0.5932%	0.0%
HQ 3,0-10	9.98% at 35.0% of the chord	2.99% at 50.0% of the chord	0.5008%	0.0%
HQ 3,0-11	10.98% at 35.0% of the chord	2.99% at 50.0% of the chord	0.6112%	0.0%
HQ 3,0-12	11.98% at 35.0% of the chord	2.99% at 50.0% of the chord	0.7458%	0.0%
HQ 3,0-13	12.99% at 35.0% of the chord	3.0% at 50.0% of the chord	0.8793%	0.0%
HQ 3,0-14	13.99% at 35.0% of the chord	2.99% at 50.0% of the chord	1.0282%	0.0%
HQ 3,0-15	14.98% at 35.0% of the chord	2.99% at 50.0% of the chord	1.1878%	0.0%
HQ 3,0-8	7.98% at 35.0% of the chord	2.99% at 50.0% of the chord	0.3254%	0.0%
HQ 3,0-9	8.98% at 35.0% of the chord	2.99% at 50.0% of the chord	0.4067%	0.0%
HQ 3,5-10	9.96% at 35.0% of the chord	3.5% at 50.0% of the chord	0.4799%	0.0%
HQ 3,5-12	11.96% at 35.0% of the chord	3.5% at 50.0% of the chord	0.7125%	0.0%
HQ 3,5-13	13.0% at 35.0% of the chord	3.5% at 50.0% of the chord	0.8515%	0.0%
HQ 3,5-14	14.0% at 35.0% of the chord	3.5% at 50.0% of the chord	1.0389%	0.0%
HQ 3,5-18	18.0% at 35.0% of the chord	3.5% at 50.0% of the chord	1.8464%	0.0%
HQ 3,5-8	7.97% at 35.0% of the chord	3.5% at 50.0% of the chord	0.3116%	0.0%
HQ 3,5-9	8.97% at 35.0% of the chord	3.5% at 50.0% of the chord	0.3886%	0.0%
HQ-00-09	8.11% at 33.9% of the chord	0.0% at 0.0% of the chord	0.4787%	0.0%
HQ-2,0-9 9,0% smoothed	8.97% at 35.0% of the chord	1.99% at 50.0% of the chord	0.3802%	0.0%
HQ-20-11	11.0% at 33.9% of the chord	2.0% at 50.0% of the chord	0.7479%	0.0%
HQ-60-20	20.0% at 33.9% of the chord	6.0% at 50.0% of the chord	2.2068%	0.0%
HS 2.0/8.0	7.99% at 30.0% of the chord	2.0% at 25.0% of the chord	0.347%	0.0%
HS 3.0/8	8.0% at 30.0% of the chord	2.97% at 30.0% of the chord	0.2611%	0.0%
HS 3.0/9.0	8.99% at 30.0% of the chord	2.94% at 30.0% of the chord	0.4474%	0.0%
HS 3.5/12	12.0% at 30.0% of the chord	3.5% at 30.0% of the chord	1.2295%	0.0%
HS 510	8.79% at 27.0% of the chord	2.19% at 27.0% of the chord	0.7213%	0.0%
HS 602	10.21% at 28.7% of the chord	2.98% at 55.7% of the chord	0.7578%	0.0%
HSNLF(1)-0213	13.25% at 42.6% of the chord	1.37% at 32.6% of the chord	0.9494%	0.134%
HT 05	4.81% at 17.1% of the chord	0.0% at 0.1% of the chord	0.5373%	0.36%
HT 08	5.0% at 20.2% of the chord	0.07% at 0.0% of the chord	0.4859%	0.3472%
HT 12	5.02% at 18.6% of the chord	0.0% at 1.7% of the chord	0.4965%	0.238%
HT22	5.08% at 19.1% of the chord	1.07% at 22.7% of the chord	0.6161%	0.163%
HT23	6.51% at 20.8% of the chord	1.08% at 22.6% of the chord	0.6993%	0.2082%
HUGHES HELICOPTERS HH-02	9.57% at 30.0% of the chord	2.02% at 40.0% of the chord	0.6722%	0.38%
hydrofoil"Profile 915"	9.09% at 35.7% of the chord	1.76% at 67.0% of the chord	0.449%	0.0%
hydrofoil"Profile 930"	9.08% at 33.6% of the chord	3.02% at 57.9% of the chord	0.5023%	0.0%

Note:
HN-832TA, HN-951, HN-956, HN-971, HN-972, HN-974, HN-975, HN-975TA, HN-980 (Planeur>3.5m, Norbert Habbe);
HN-785SR, HN-805 (F3F Norbert Habbe);
HN-785, HN-981, HN-989, HN-990 (F3B Norbert Habbe);
HN-979, HN979D, HN-997A, HN-997B, HN-998, HN-999 (HLG Norbert Habbe);
HN-464 (Planeur Norbert Habbe);
HN-961SA, HN-976S (Aile volante Norbert Habbe);
HN-465, HN-973 (F3J Norbert Habbe);
HN-801 (BASIC Norbert Habbe);
HN-808, HN-832 (Planeur<3.5m, Norbert Habbe);

Hobie Hawk (Hobie Hawk R/C sailplane);
HQ 2,0-13, HQ 2,5-14 (Elaborato da Profili 1.2);
HS 2.0/8.0, HS 3.0/8, HS 3.0/9.0, HS 3.5/12, HS 510, HS 602 (Hartmut Siegmann);
HT 05 (Tail section Apogee HLG series Molded Wing C);
HT 08 (Allegro 2m tail section 1 Mark Drela);
HT 12 (Allegro 2m tail section 2 Mark Drela);
HT22, HT23 (SuperGee RC DLG by Mark Drela);
hydrofoil"Profile 915", hydrofoil"Profile 930" (Johannes Schoon).

Table 2. The geometric shapes of the airfoils in the cross section.

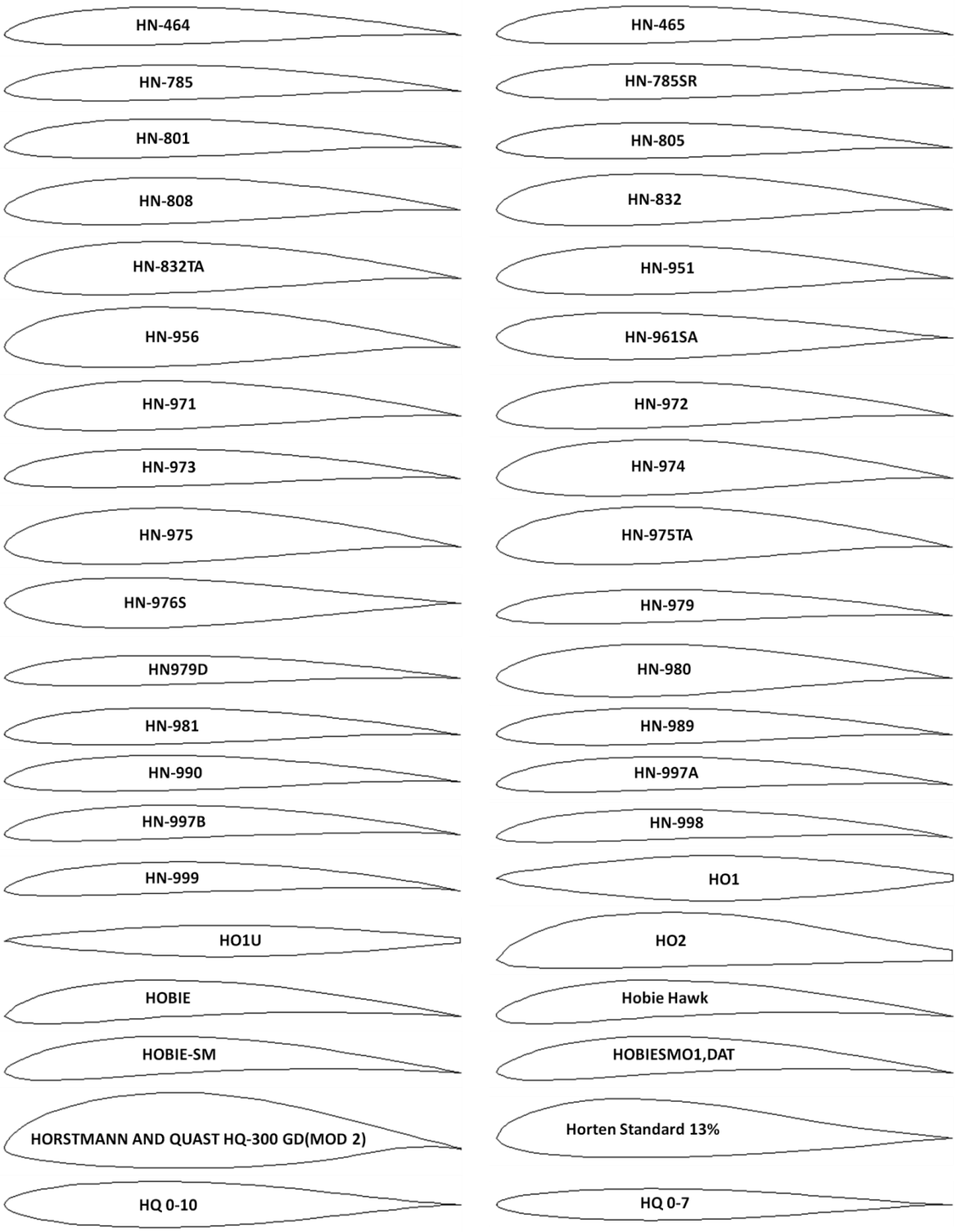

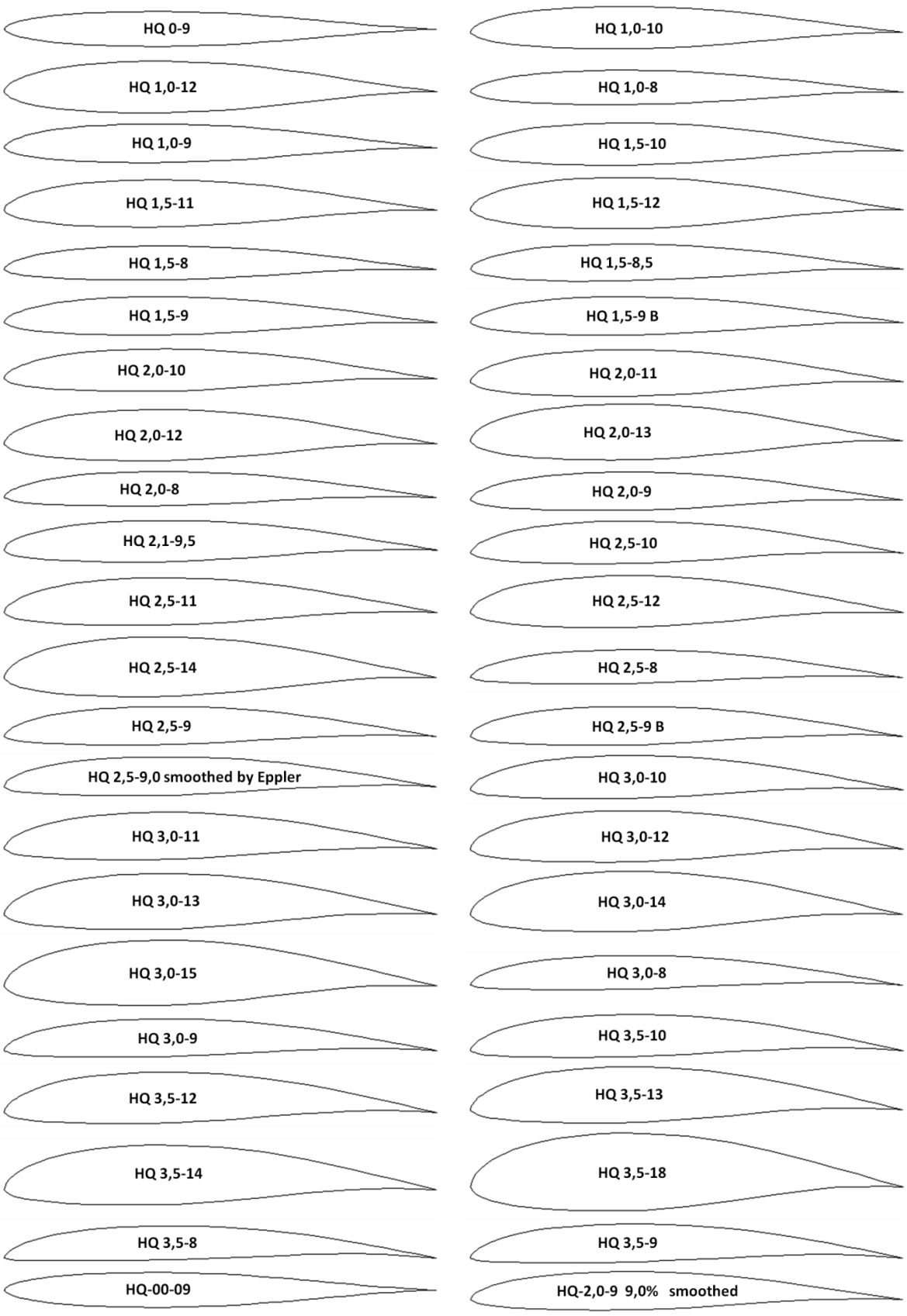
HQ 0-9
HQ 1,0-10
HQ 1,0-12
HQ 1,0-8
HQ 1,0-9
HQ 1,5-10
HQ 1,5-11
HQ 1,5-12
HQ 1,5-8
HQ 1,5-8,5
HQ 1,5-9
HQ 1,5-9 B
HQ 2,0-10
HQ 2,0-11
HQ 2,0-12
HQ 2,0-13
HQ 2,0-8
HQ 2,0-9
HQ 2,1-9,5
HQ 2,5-10
HQ 2,5-11
HQ 2,5-12
HQ 2,5-14
HQ 2,5-8
HQ 2,5-9
HQ 2,5-9 B
HQ 2,5-9,0 smoothed by Eppler
HQ 3,0-10
HQ 3,0-11
HQ 3,0-12
HQ 3,0-13
HQ 3,0-14
HQ 3,0-15
HQ 3,0-8
HQ 3,0-9
HQ 3,5-10
HQ 3,5-12
HQ 3,5-13
HQ 3,5-14
HQ 3,5-18
HQ 3,5-8
HQ 3,5-9
HQ-00-09
HQ-2,0-9 9,0% smoothed

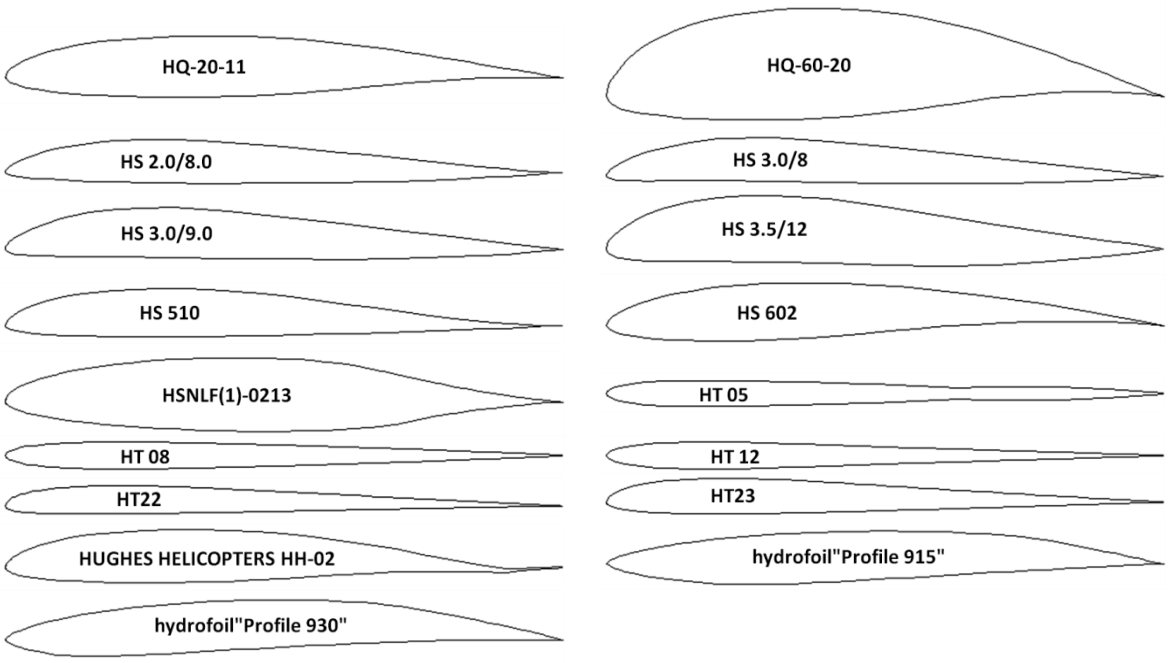

Results and discussion

The calculated pressure contours on the surfaces of the airfoils at the different angles of attack are presented in the Figs. 1-101.

The calculated values on the scale can be represented as the basic values when comparing the pressure drop under conditions of changing the angle of attack of the airfoils.

In this work, 99 airfoils and 2 hydrofoils of the HN, HQ, HT, HS, etc. series were studied. The airfoils are represented by asymmetrical geometries and symmetrical geometries (HN-976S, HQ 0-10, HQ 0-7, HQ 0-9, HQ-00-09, HT 05 and HT 12) in the cross section.

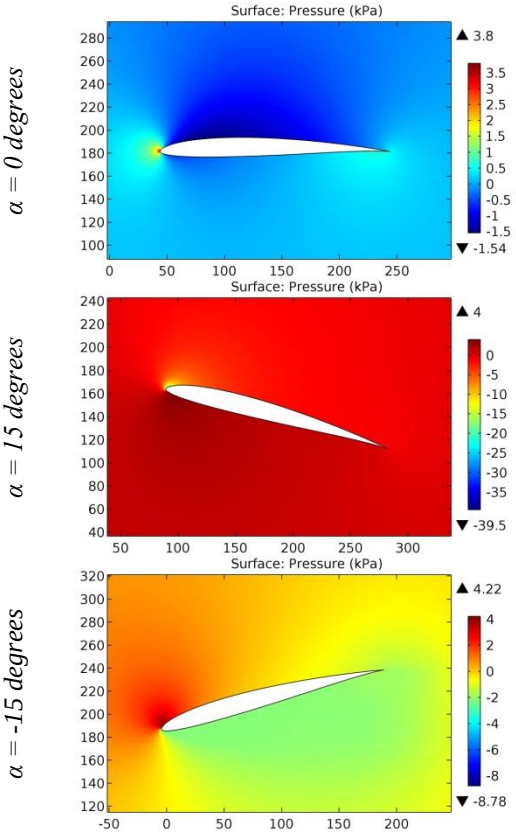

Figure 1. The pressure contours on the surfaces of the HN-464 airfoil.

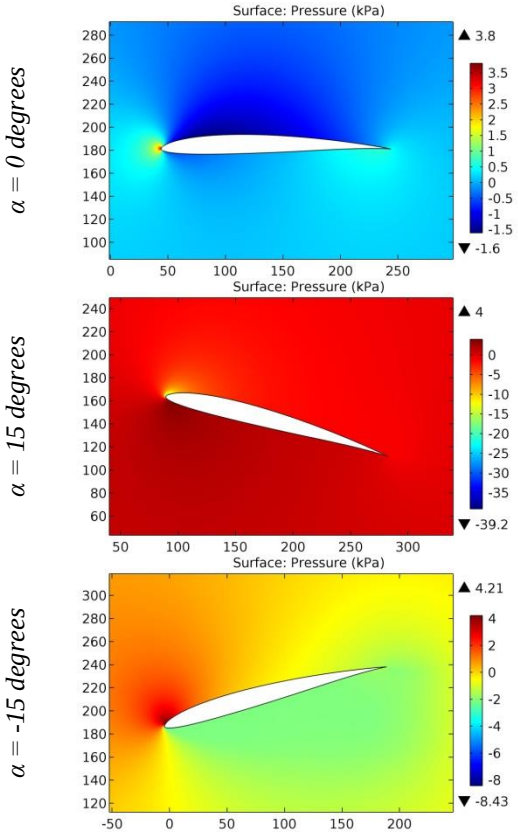

Figure 2. The pressure contours on the surfaces of the HN-465 airfoil.

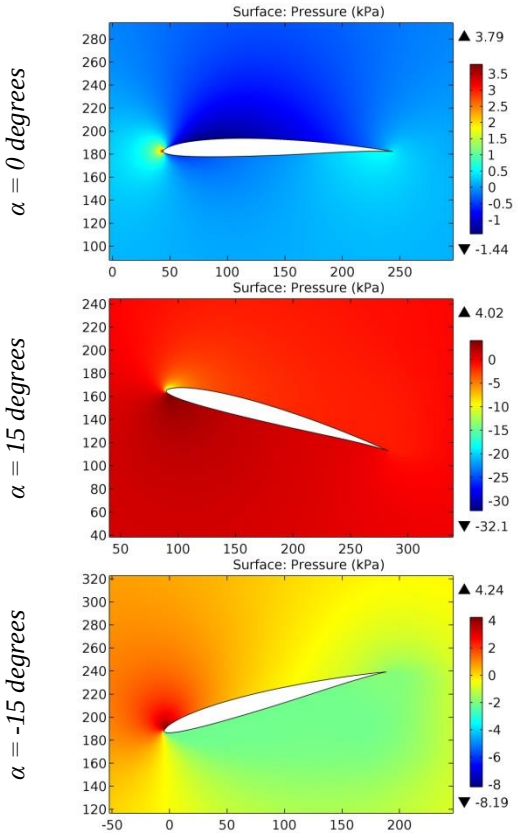

Figure 3. The pressure contours on the surfaces of the HN-785 airfoil.

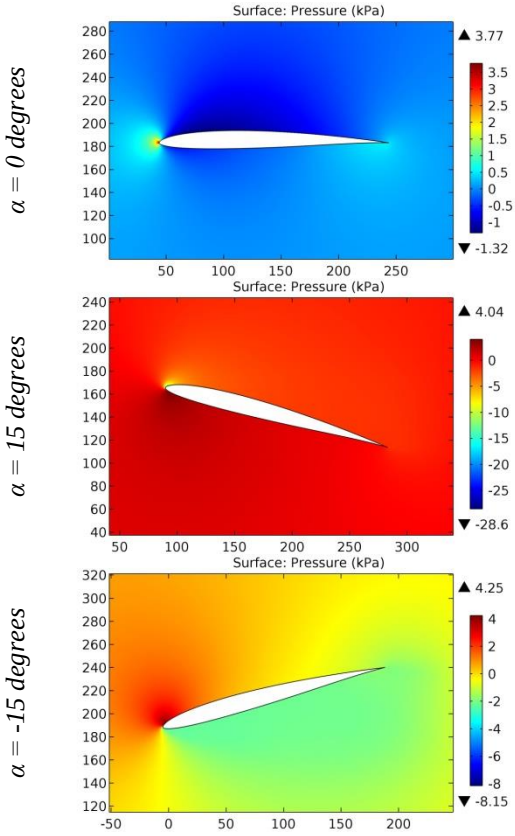

Figure 4. The pressure contours on the surfaces of the HN-785SR airfoil.

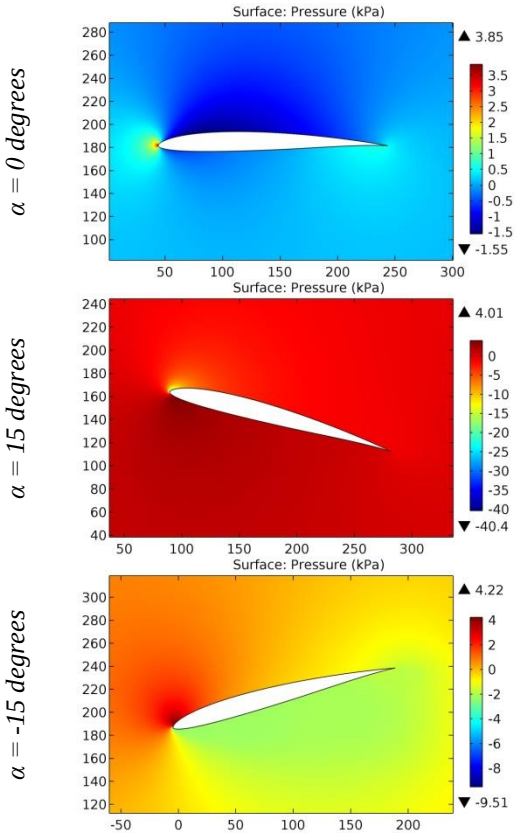

Figure 5. The pressure contours on the surfaces of the HN-801 airfoil.

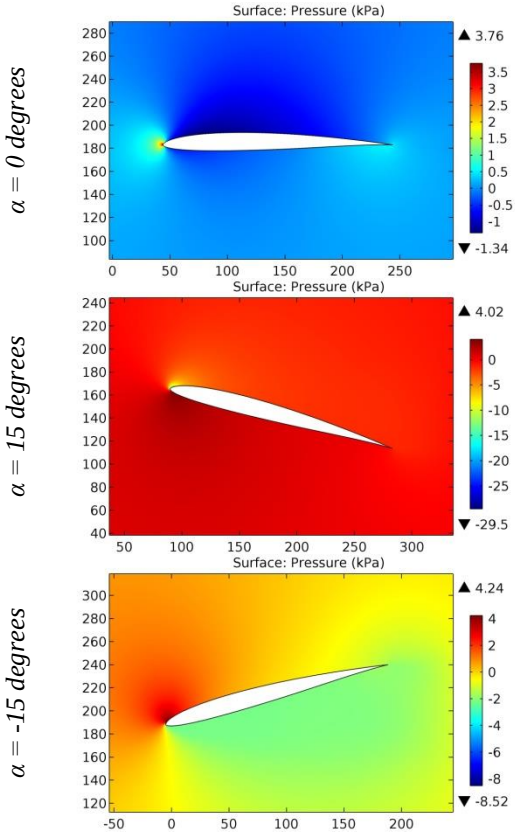

Figure 6. The pressure contours on the surfaces of the HN-805 airfoil.

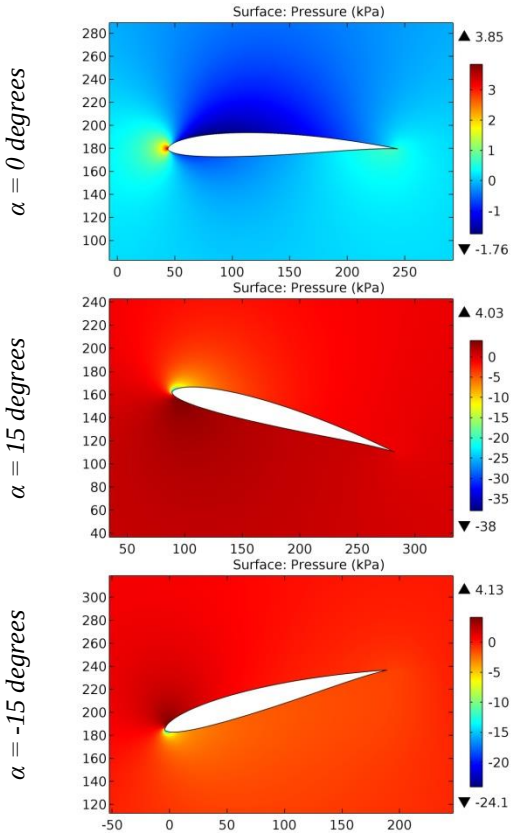

Figure 7. The pressure contours on the surfaces of the HN-808 airfoil.

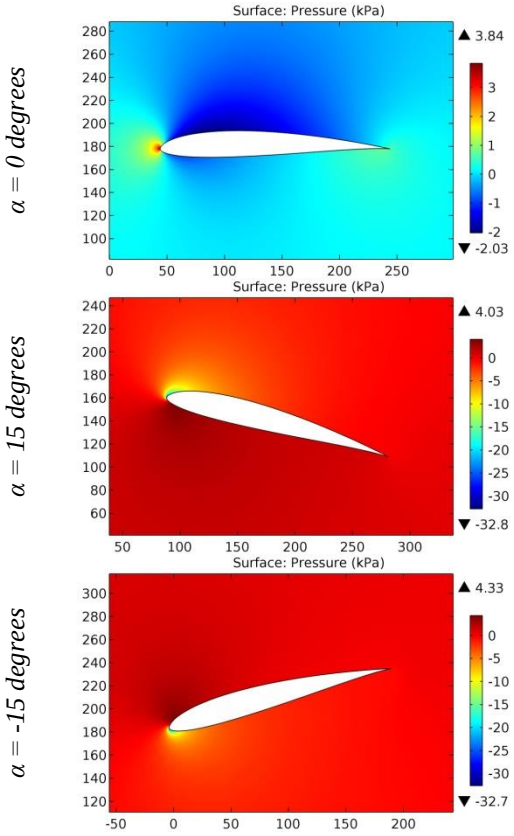

Figure 8. The pressure contours on the surfaces of the HN-832 airfoil.

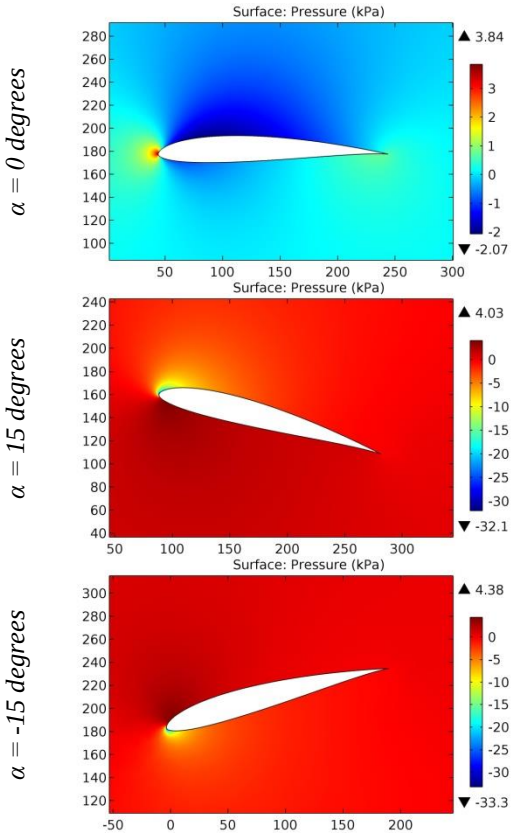

Figure 9. The pressure contours on the surfaces of the HN-832TA airfoil.

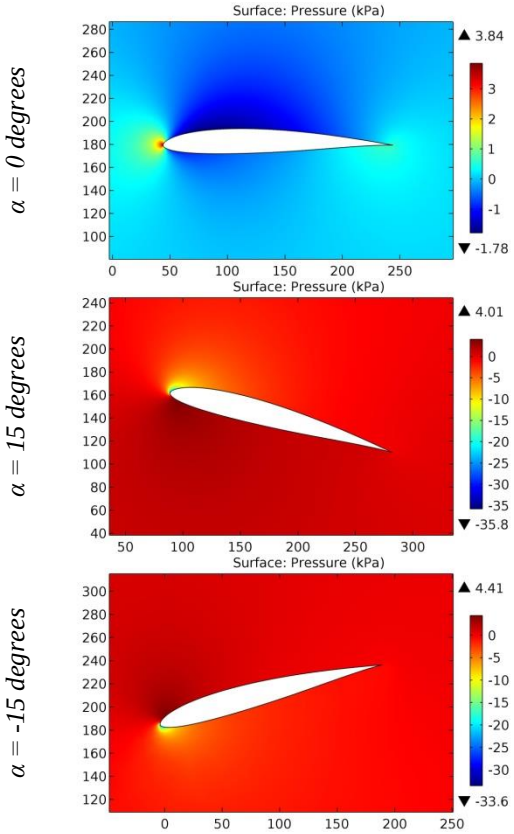

Figure 10. The pressure contours on the surfaces of the HN-951 airfoil.

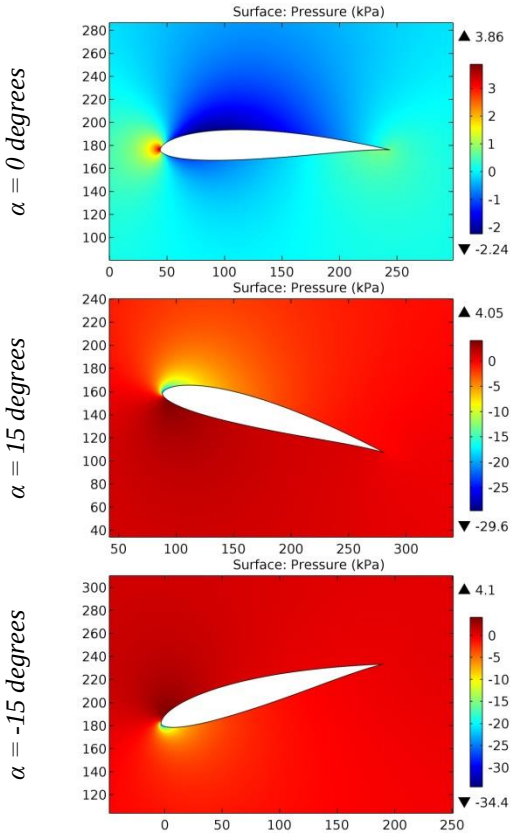

Figure 11. The pressure contours on the surfaces of the HN-956 airfoil.

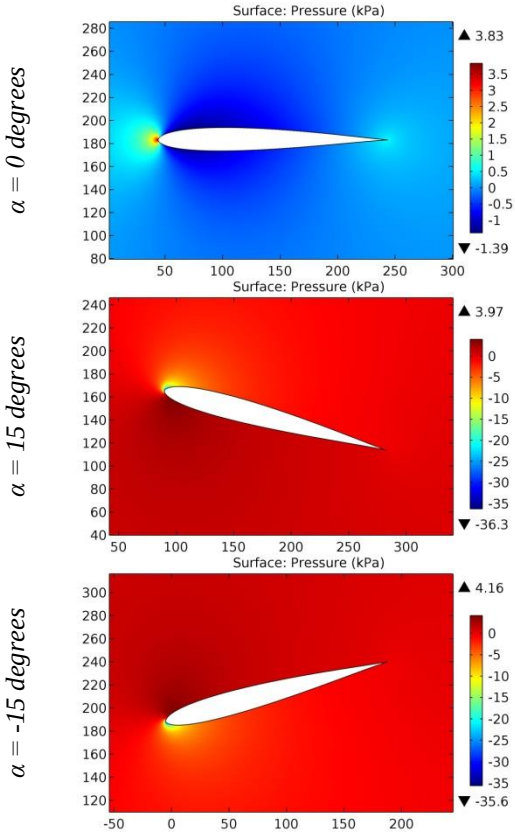

Figure 12. The pressure contours on the surfaces of the HN-961SA airfoil.

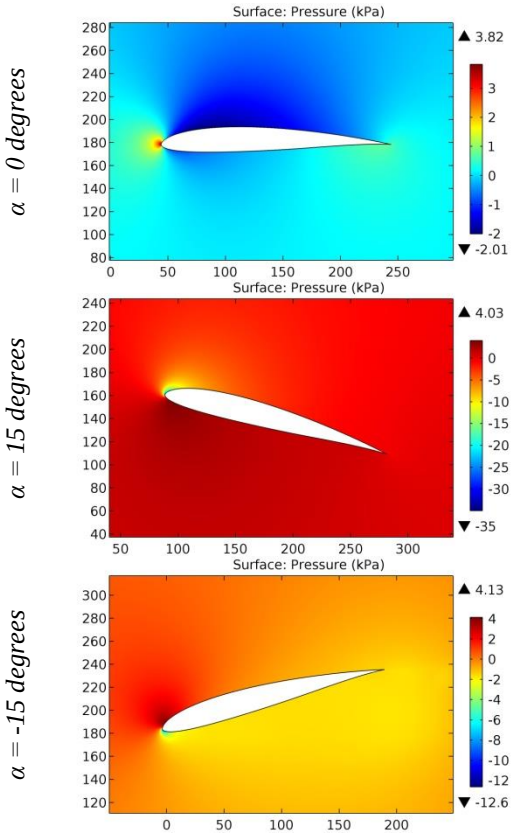

Figure 13. The pressure contours on the surfaces of the HN-971 airfoil.

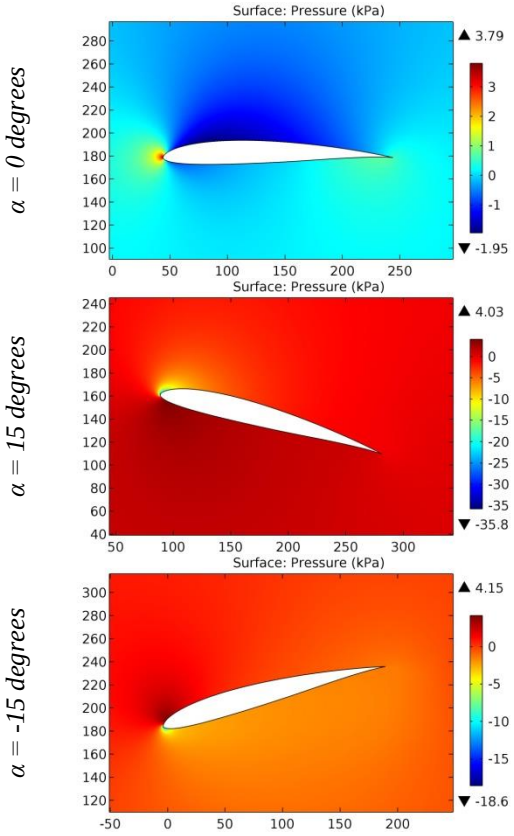

Figure 14. The pressure contours on the surfaces of the HN-972 airfoil.

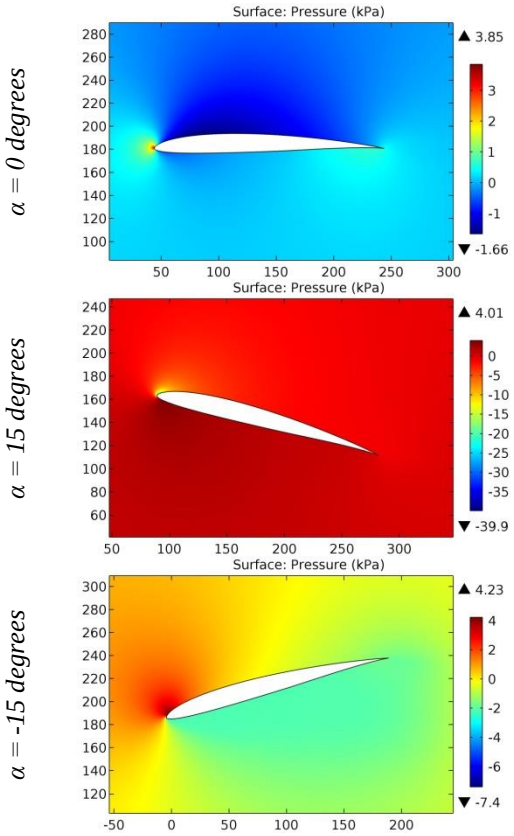

Figure 15. The pressure contours on the surfaces of the HN-973 airfoil.

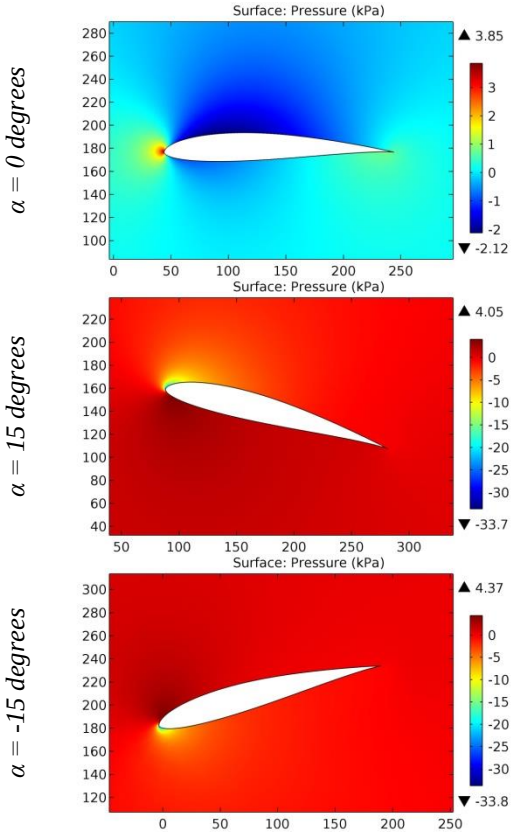

Figure 16. The pressure contours on the surfaces of the HN-974 airfoil.

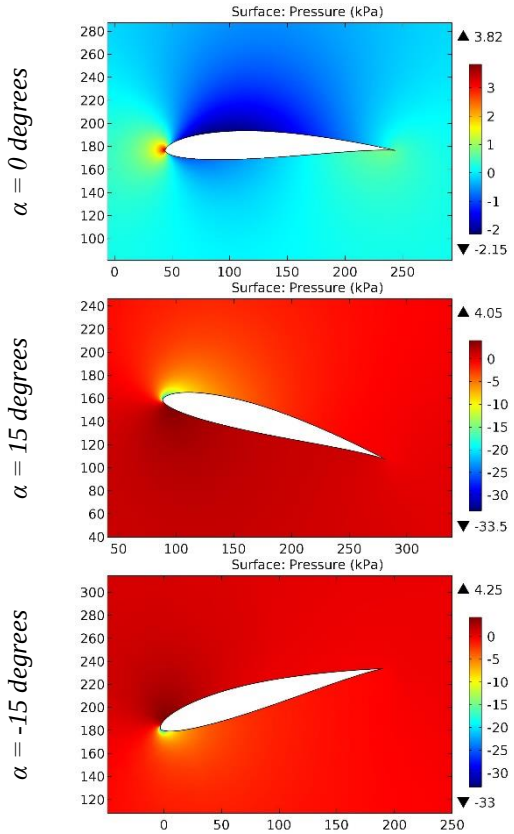

Figure 17. The pressure contours on the surfaces of the HN-975 airfoil.

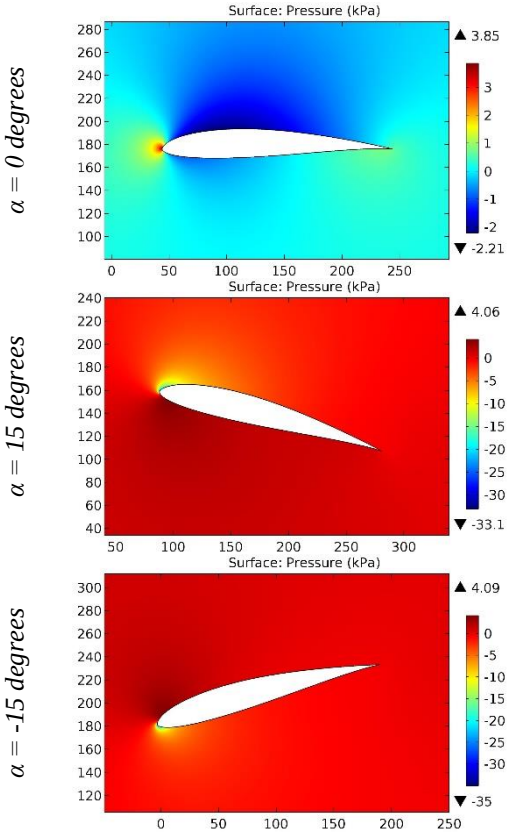

Figure 18. The pressure contours on the surfaces of the HN-975TA airfoil.

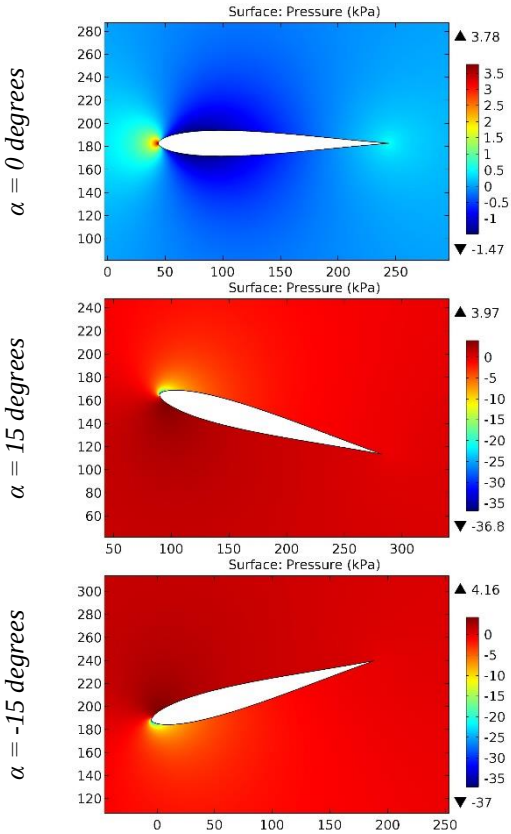

Figure 19. The pressure contours on the surfaces of the HN-976S airfoil.

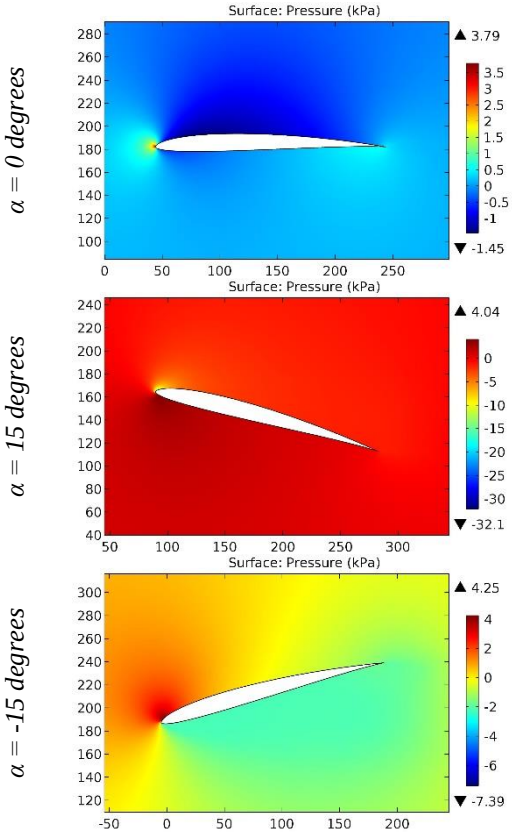

Figure 20. The pressure contours on the surfaces of the HN-979 airfoil.

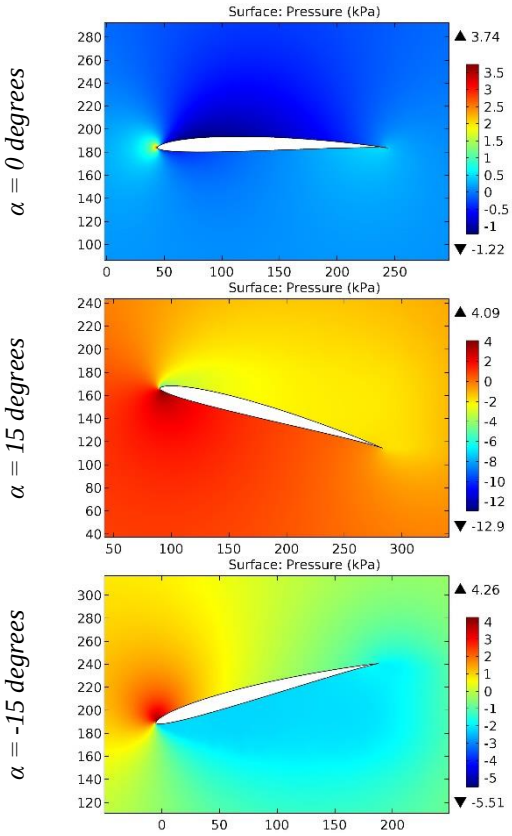

Figure 21. The pressure contours on the surfaces of the HN979D airfoil.

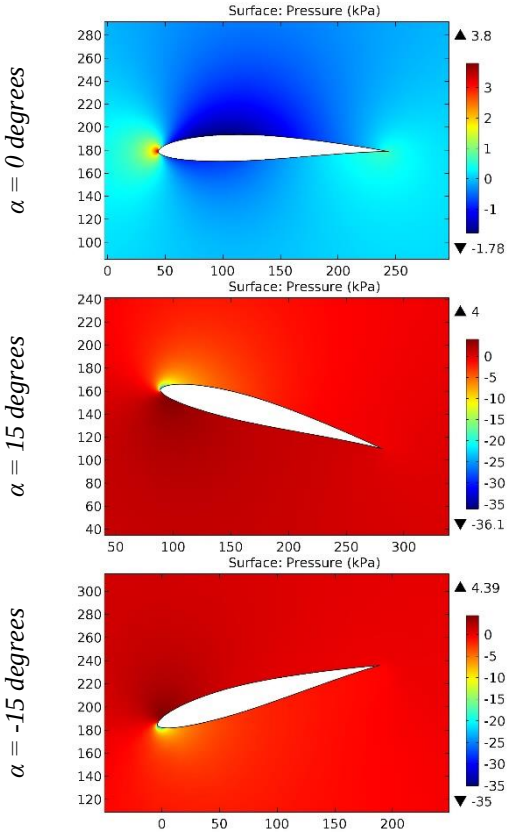

Figure 22. The pressure contours on the surfaces of the HN-980 airfoil.

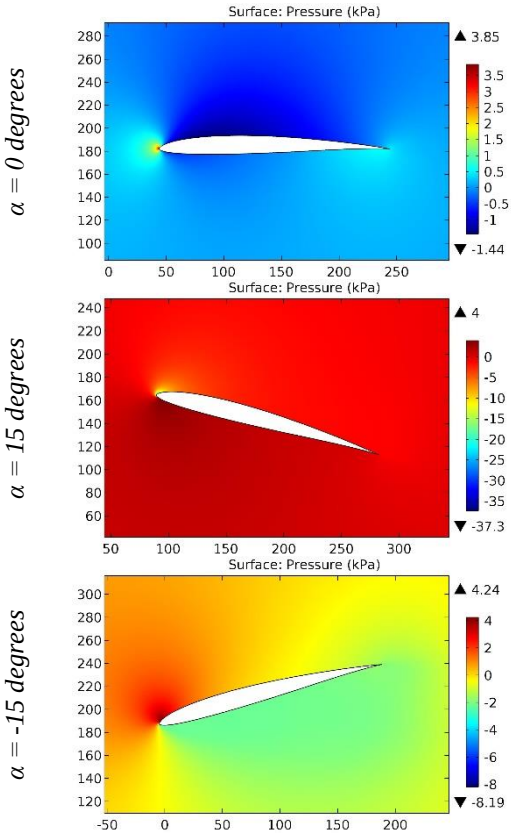

Figure 23. The pressure contours on the surfaces of the HN-981 airfoil.

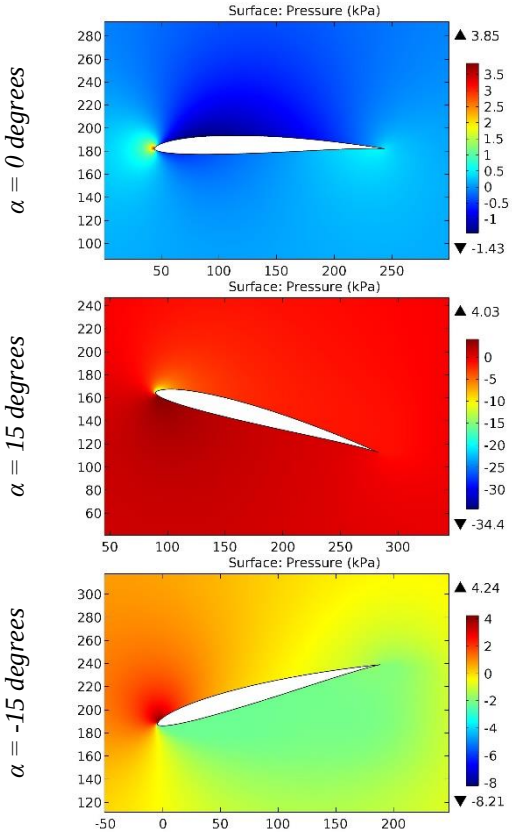

Figure 24. The pressure contours on the surfaces of the HN-989 airfoil.

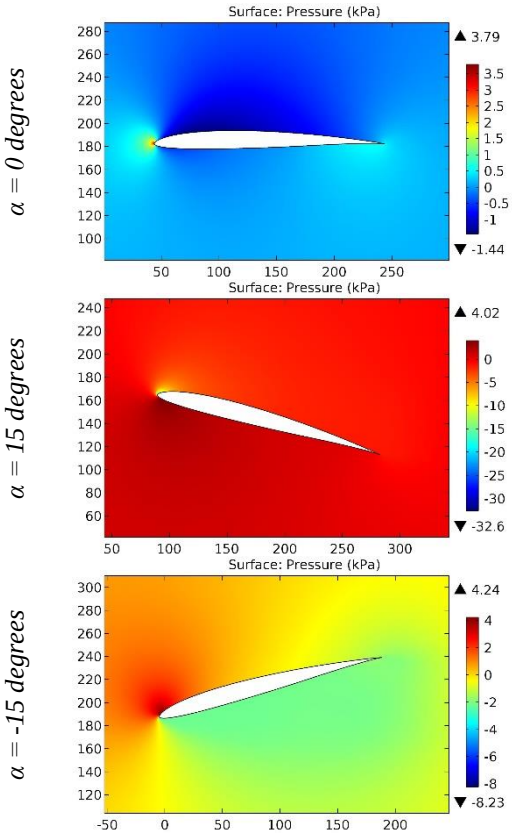

Figure 25. The pressure contours on the surfaces of the HN-990 airfoil.

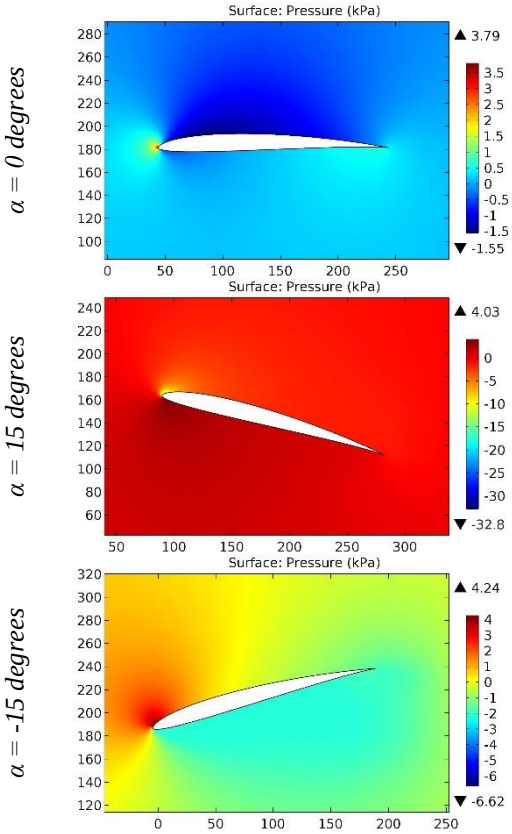

Figure 26. The pressure contours on the surfaces of the HN-997A airfoil.

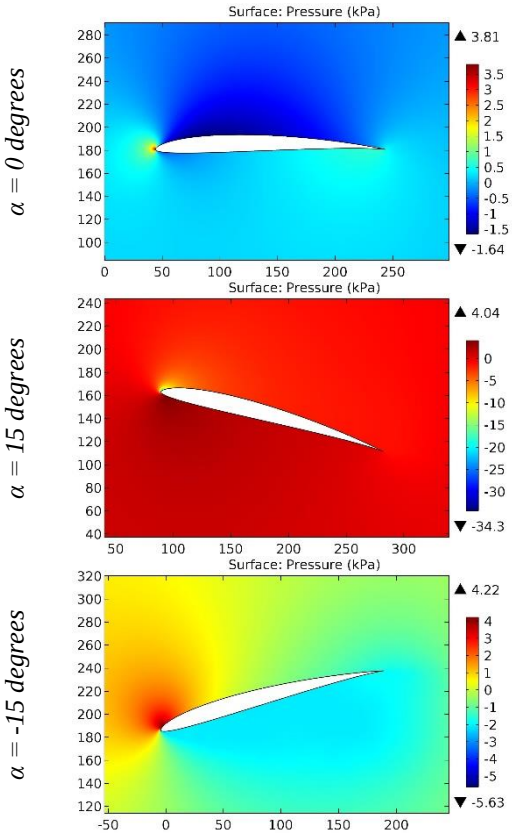

Figure 27. The pressure contours on the surfaces of the HN-997B airfoil.

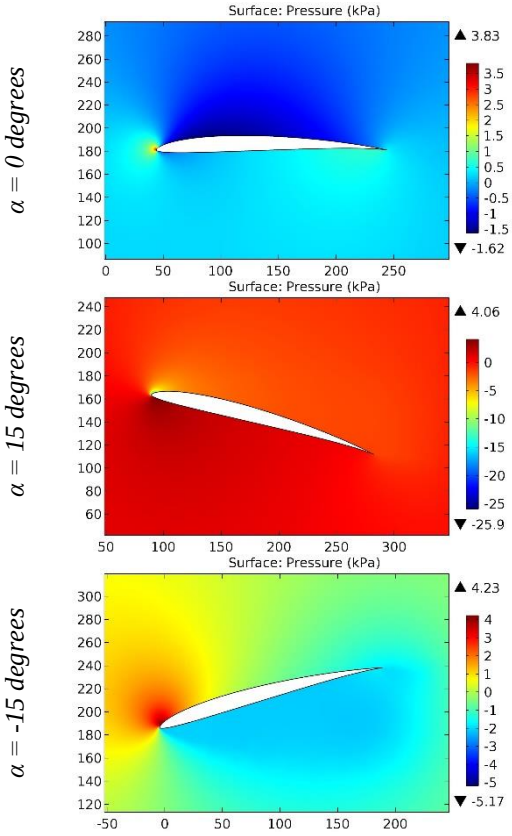

Figure 28. The pressure contours on the surfaces of the HN-998 airfoil.

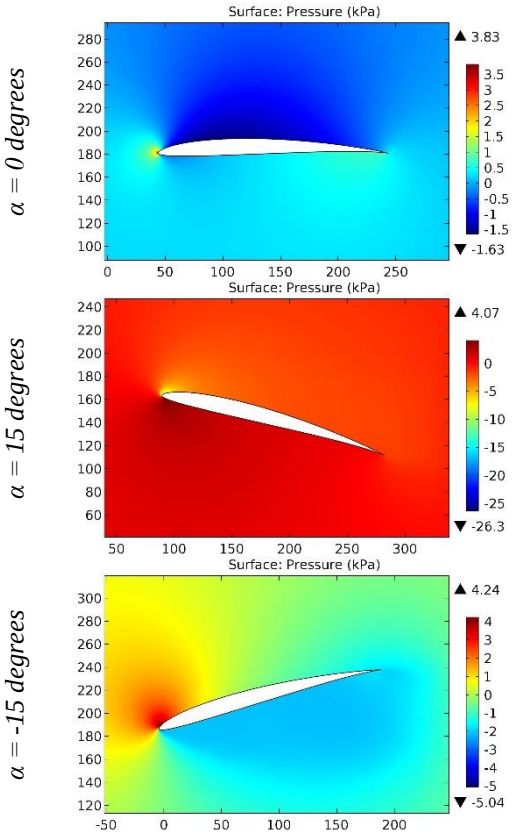

Figure 29. The pressure contours on the surfaces of the HN-999 airfoil.

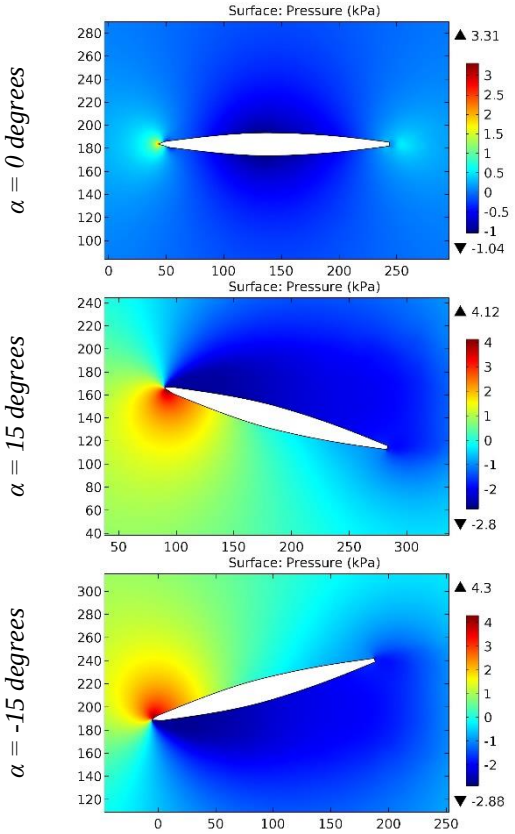

Figure 30. The pressure contours on the surfaces of the HO1 airfoil.

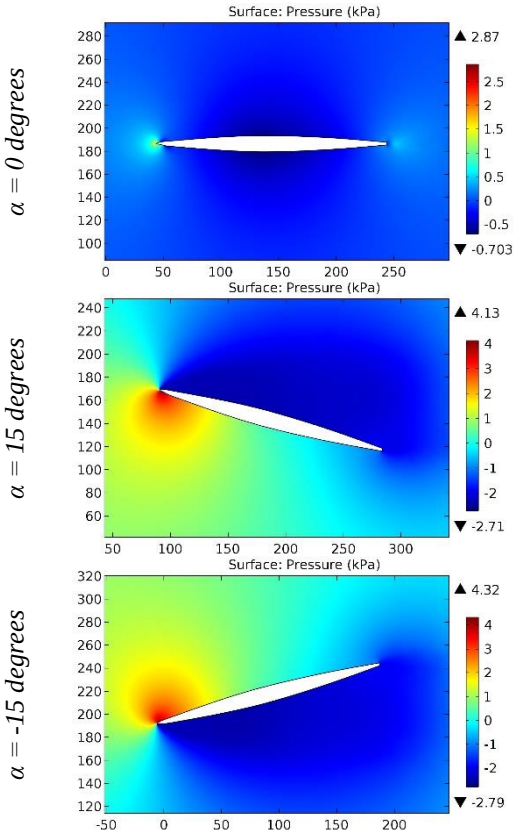

Figure 31. The pressure contours on the surfaces of the HO1U airfoil.

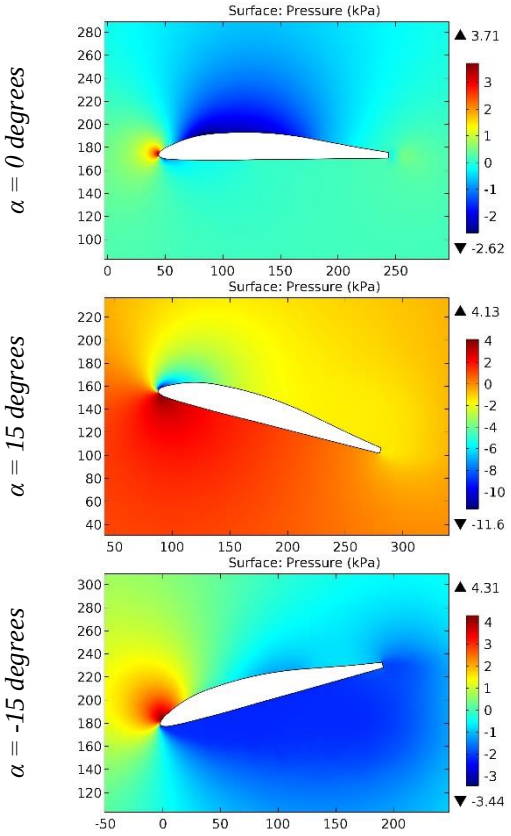

Figure 32. The pressure contours on the surfaces of the HO2 airfoil.

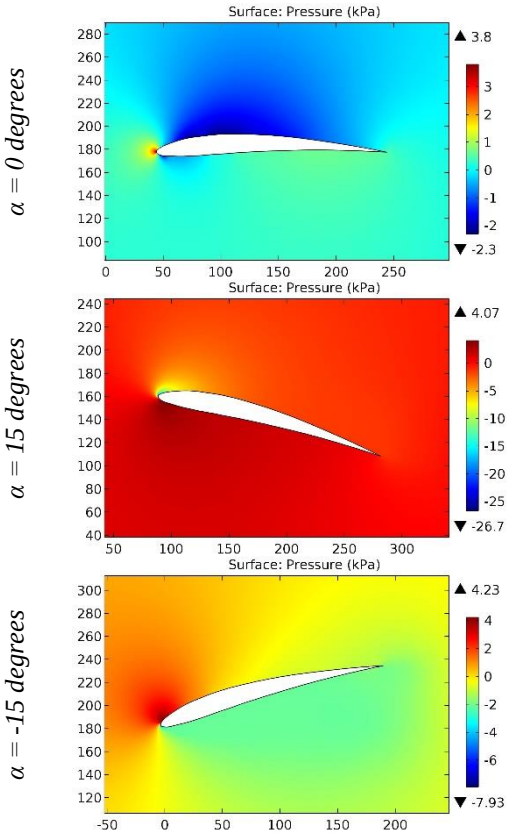

Figure 33. The pressure contours on the surfaces of the HOBIE airfoil.

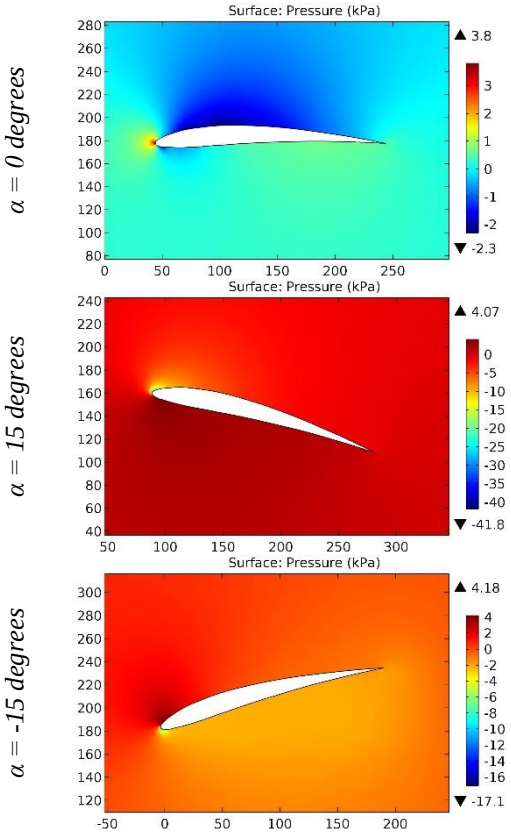

Figure 34. The pressure contours on the surfaces of the Hobie Hawk airfoil.

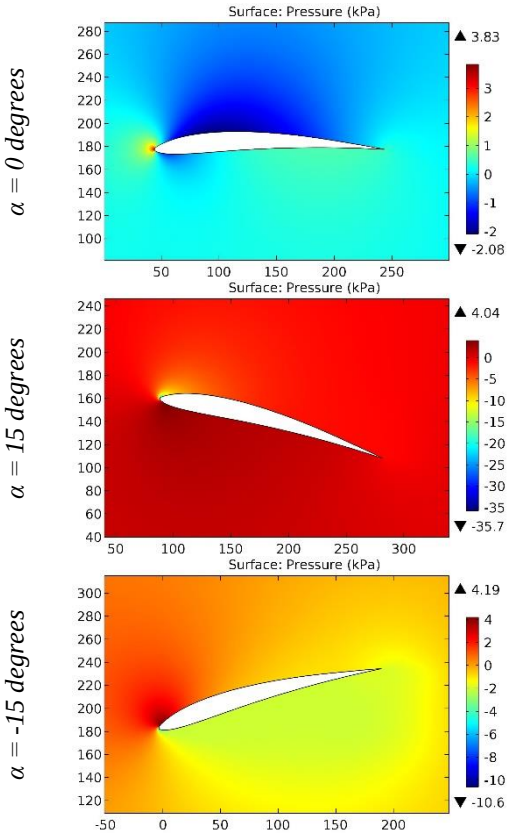

Figure 35. The pressure contours on the surfaces of the HOBIE-SM airfoil.

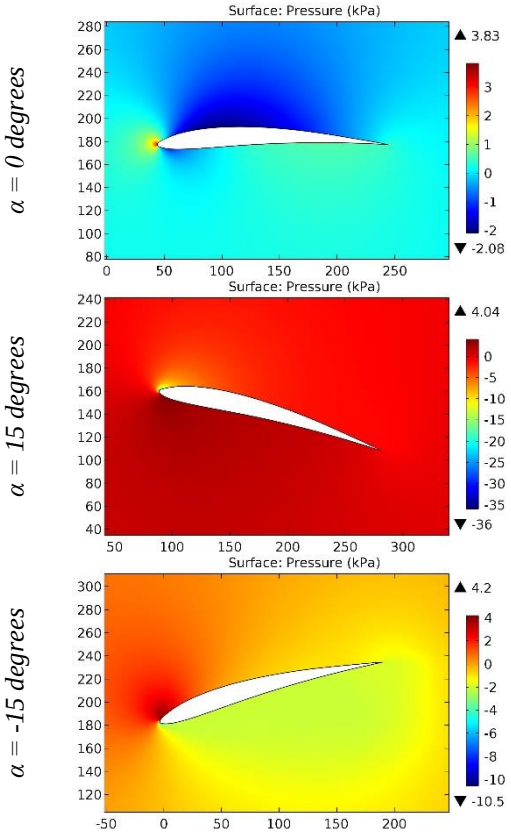

Figure 36. The pressure contours on the surfaces of the HOBIESMO1,DAT airfoil.

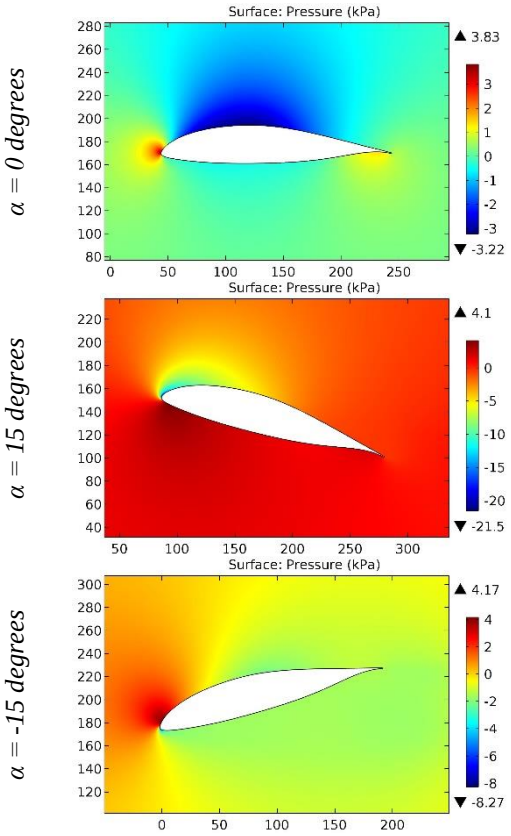

Figure 37. The pressure contours on the surfaces of the HORSTMANN AND QUAST HQ-300 GD(MOD 2) airfoil.

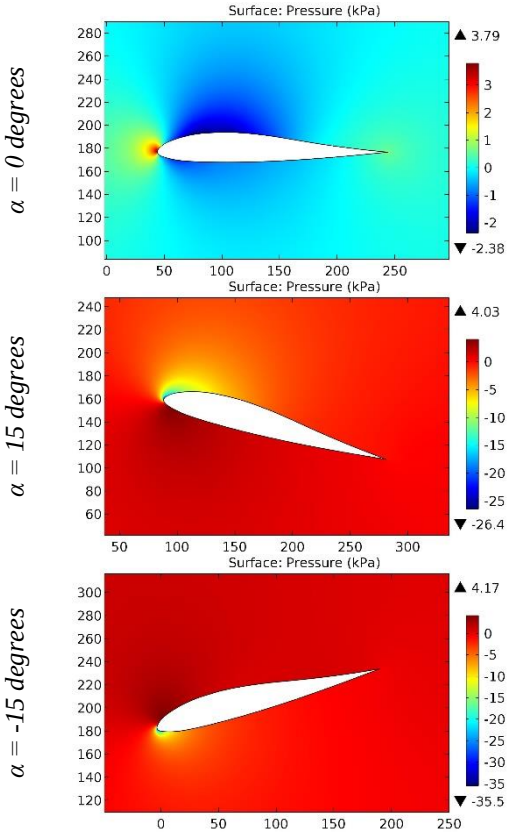

Figure 38. The pressure contours on the surfaces of the Horten Standard 13% airfoil.

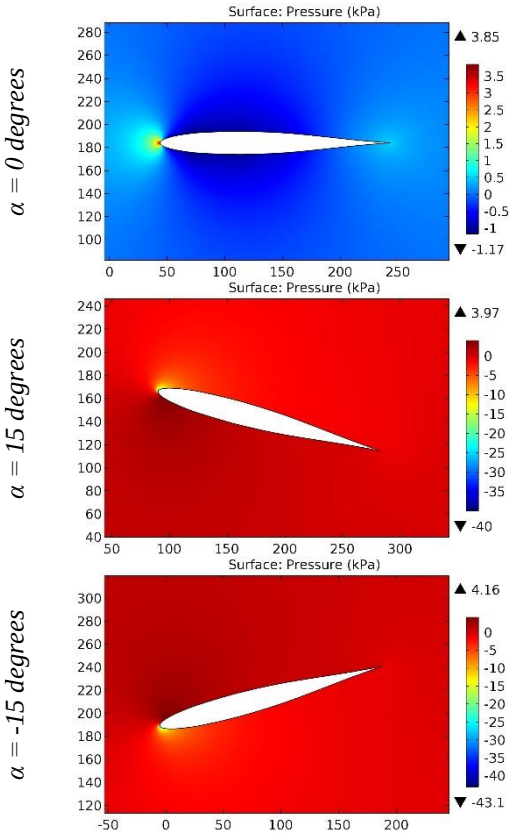

Figure 39. The pressure contours on the surfaces of the HQ 0-10 airfoil.

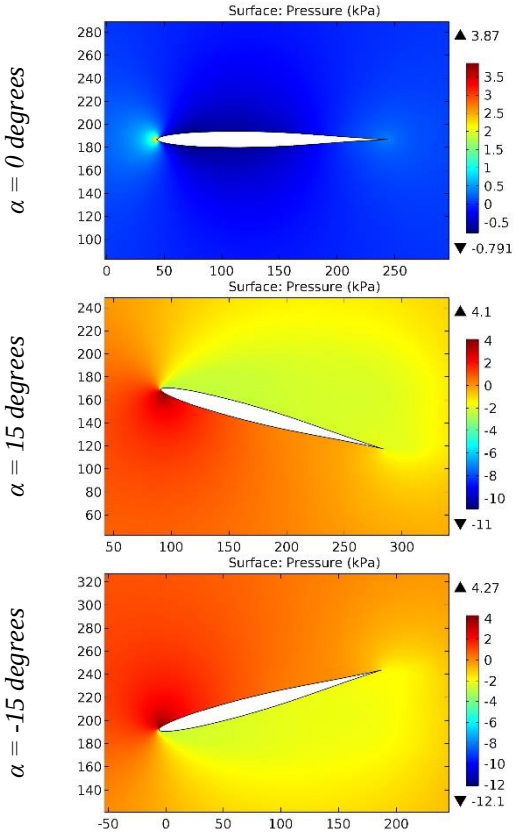

Figure 40. The pressure contours on the surfaces of the HQ 0-7 airfoil.

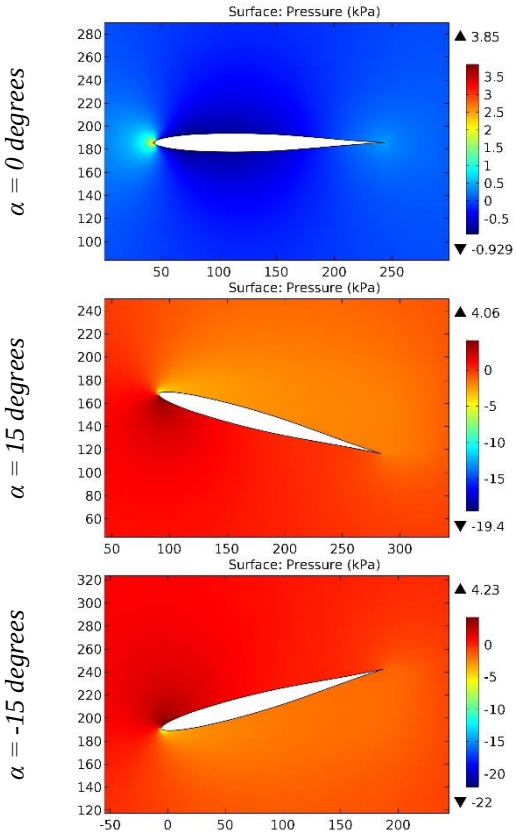

Figure 41. The pressure contours on the surfaces of the HQ 0-9 airfoil.

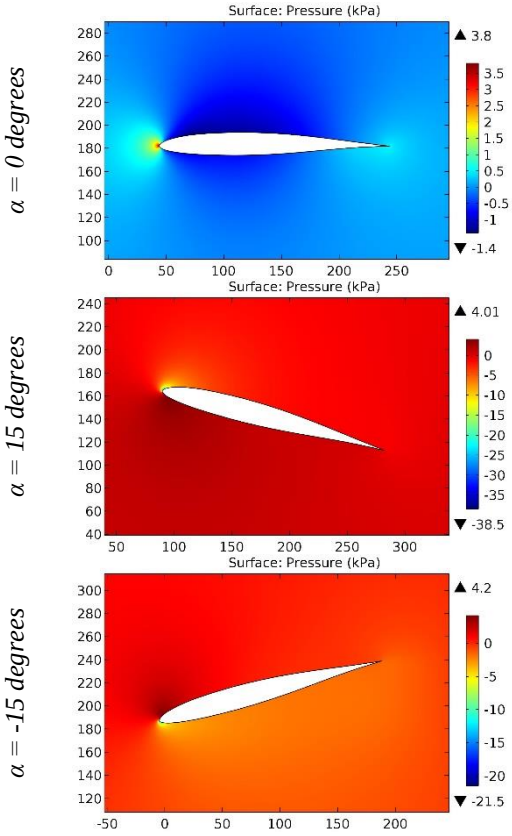

Figure 42. The pressure contours on the surfaces of the HQ 1,0-10 airfoil.

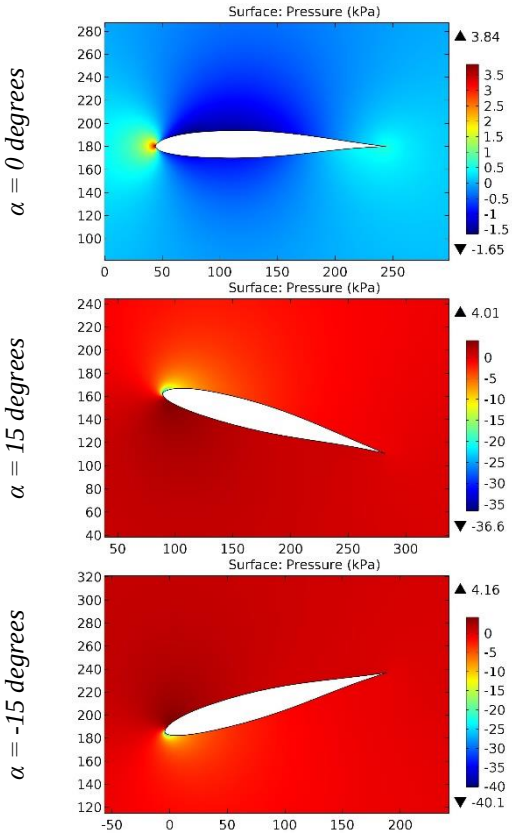

Figure 43. The pressure contours on the surfaces of the HQ 1,0-12 airfoil.

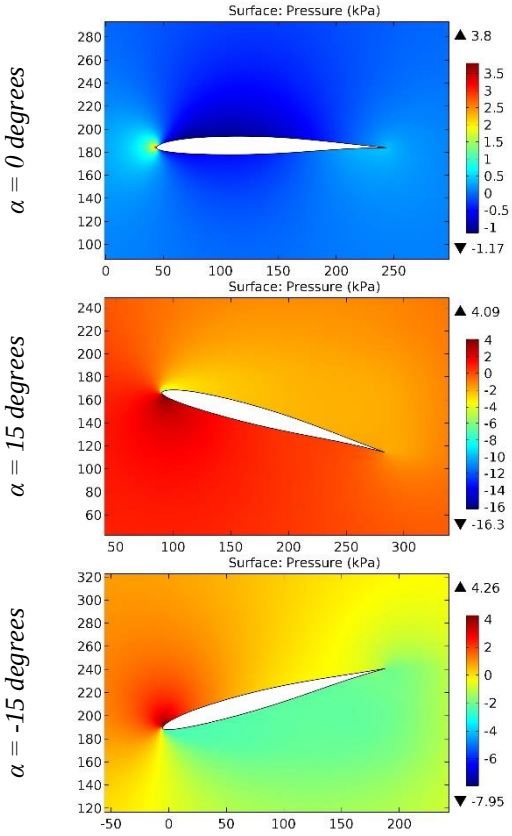

Figure 44. The pressure contours on the surfaces of the HQ 1,0-8 airfoil.

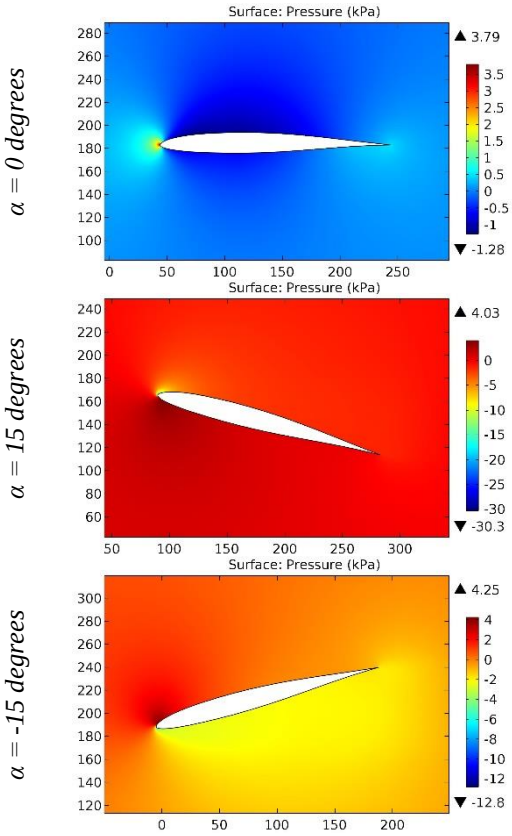

Figure 45. The pressure contours on the surfaces of the HQ 1,0-9 airfoil.

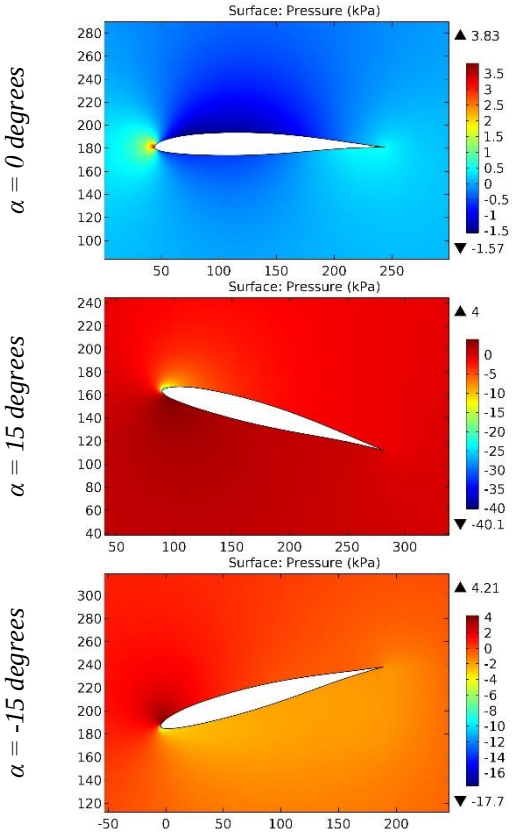

Figure 46. The pressure contours on the surfaces of the HQ 1,5-10 airfoil.

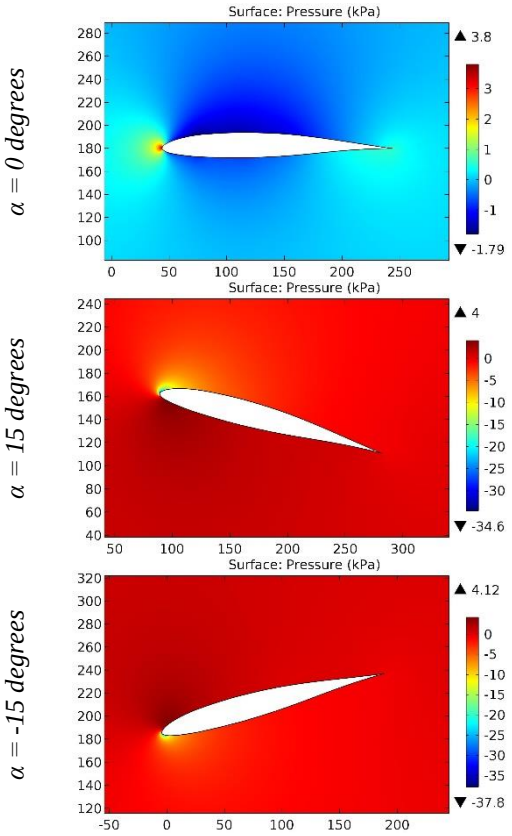

Figure 47. The pressure contours on the surfaces of the HQ 1,5-11 airfoil.

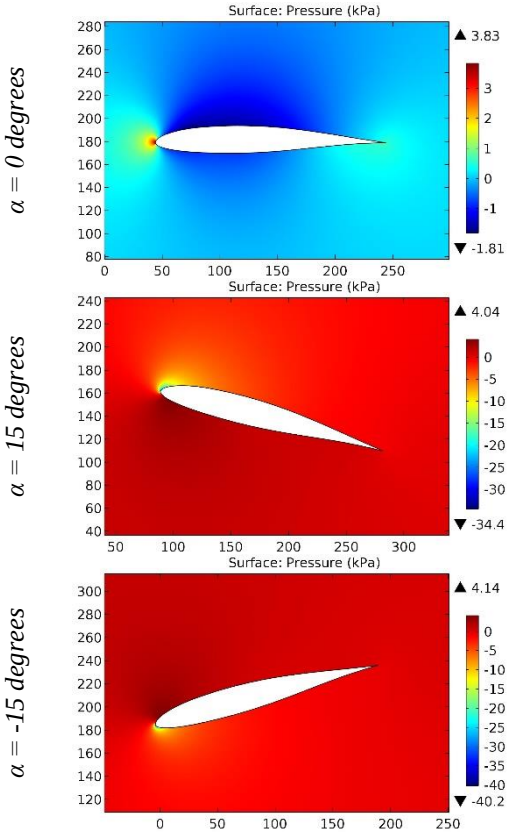

Figure 48. The pressure contours on the surfaces of the HQ 1,5-12 airfoil.

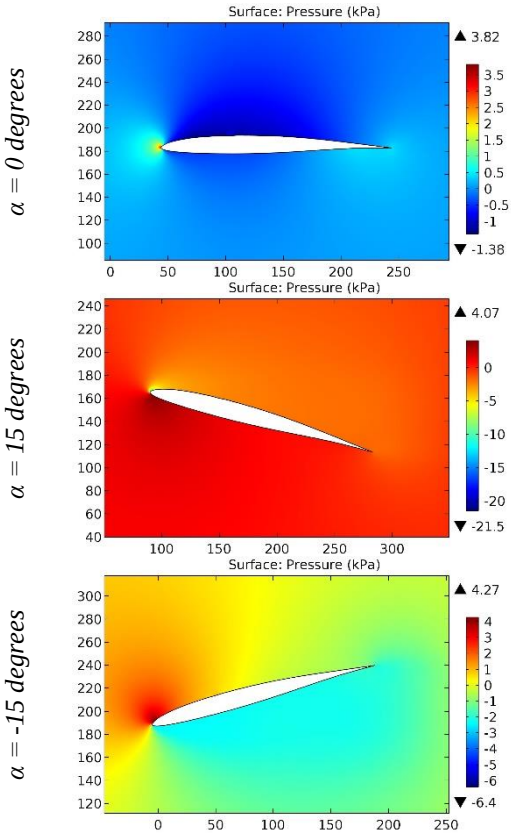

Figure 49. The pressure contours on the surfaces of the HQ 1,5-8 airfoil.

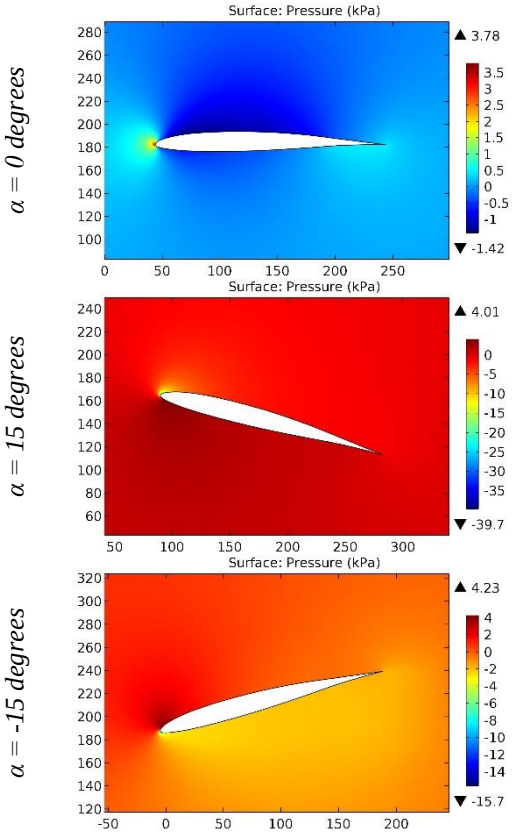

Figure 50. The pressure contours on the surfaces of the HQ 1,5-8,5 airfoil.

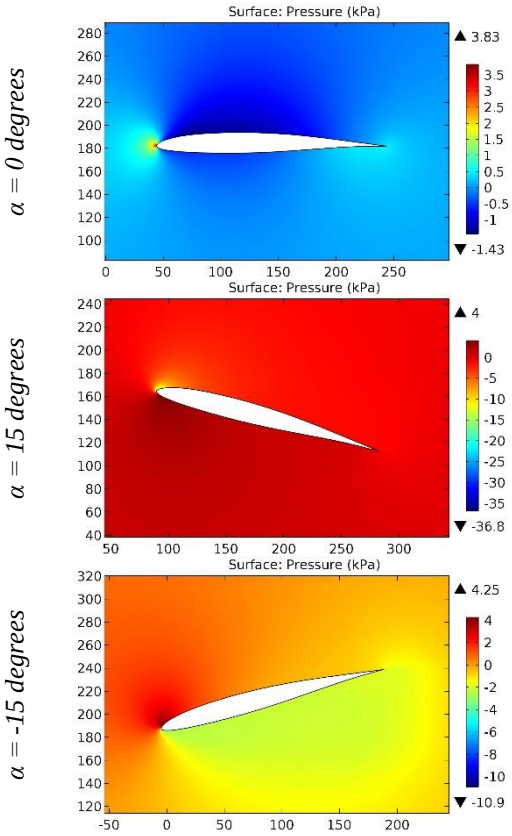

Figure 51. The pressure contours on the surfaces of the HQ 1,5-9 airfoil.

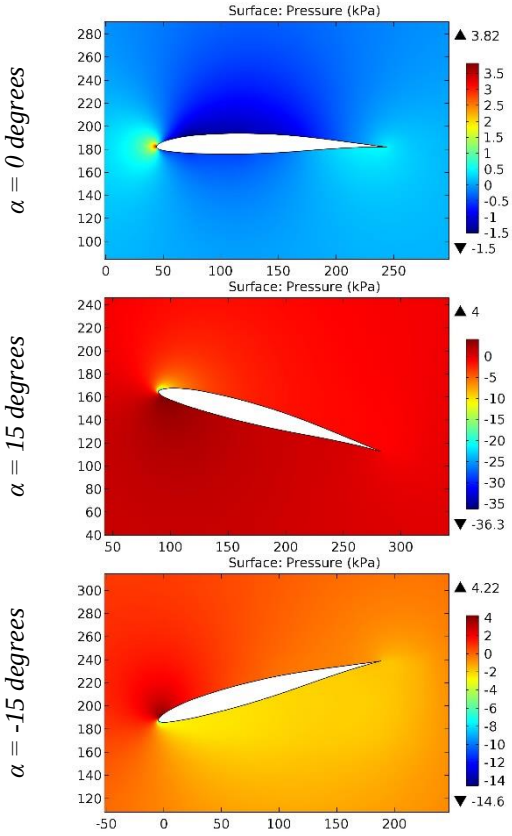

Figure 52. The pressure contours on the surfaces of the HQ 1,5-9 B airfoil.

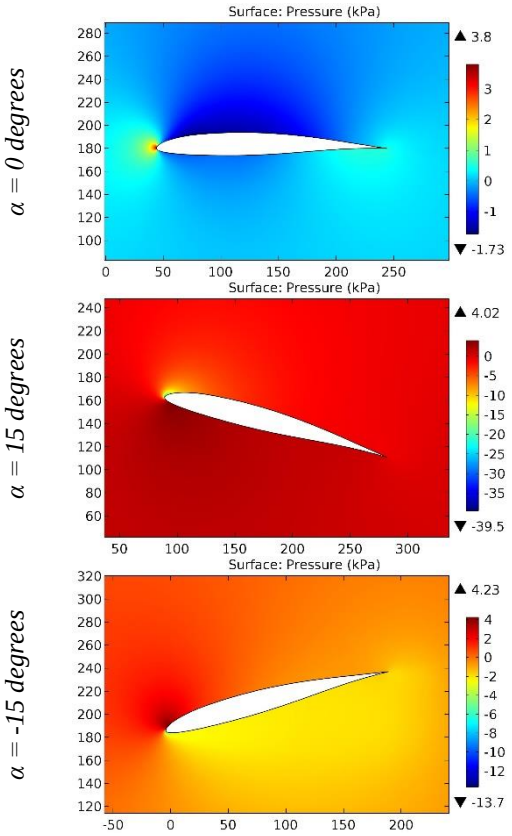

Figure 53. The pressure contours on the surfaces of the HQ 2,0-10 airfoil.

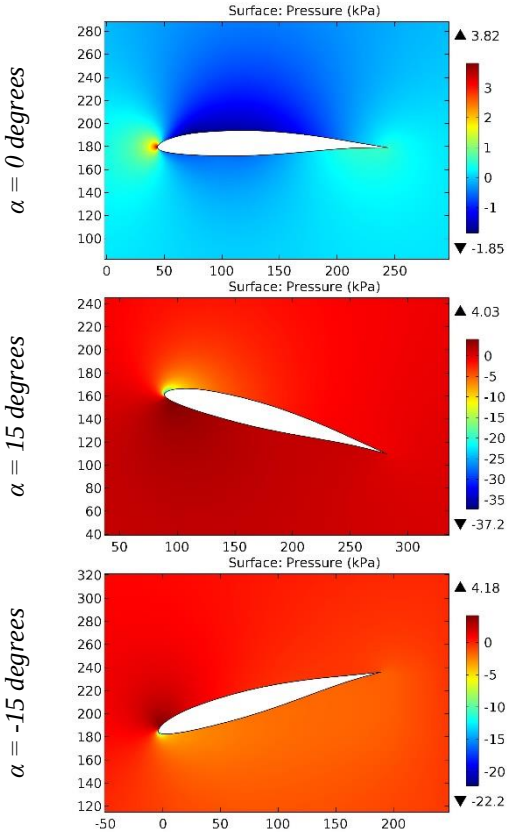

Figure 54. The pressure contours on the surfaces of the HQ 2,0-11 airfoil.

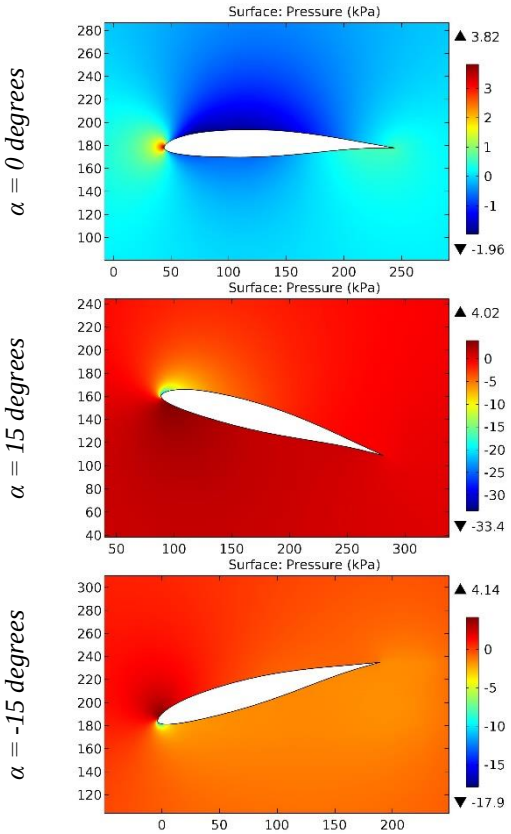

Figure 55. The pressure contours on the surfaces of the HQ 2,0-12 airfoil.

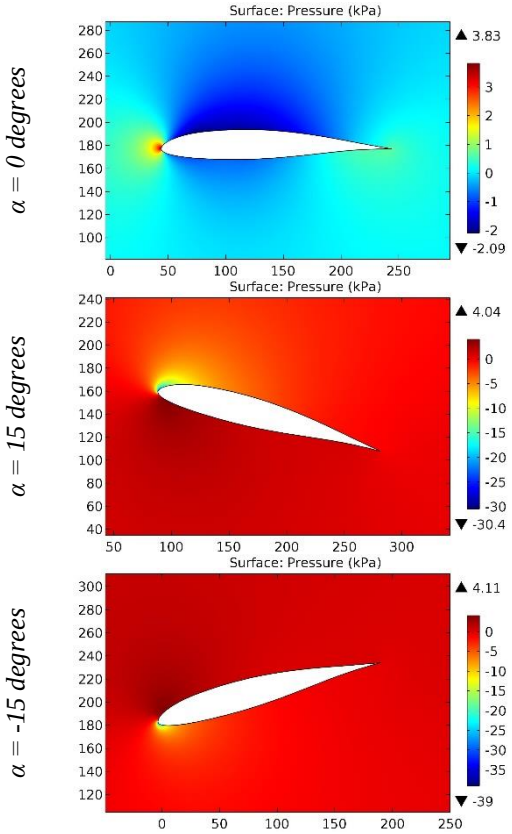

Figure 56. The pressure contours on the surfaces of the HQ 2,0-13 airfoil.

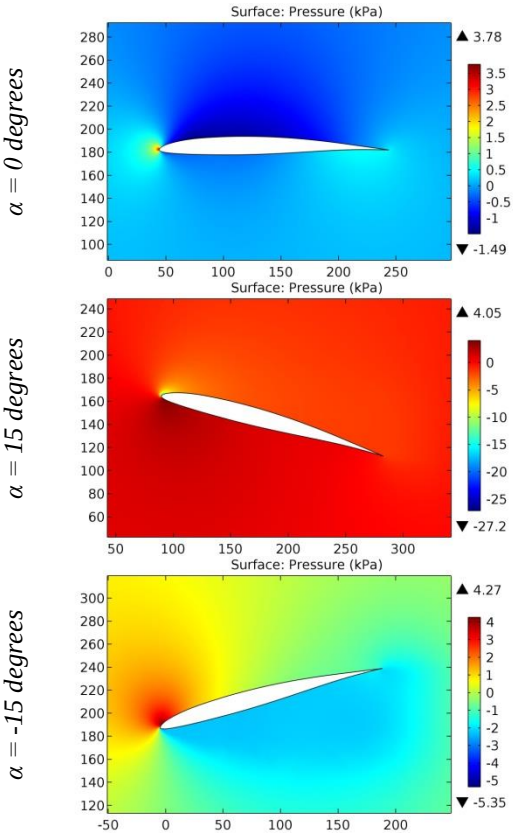

Figure 57. The pressure contours on the surfaces of the HQ 2,0-8 airfoil.

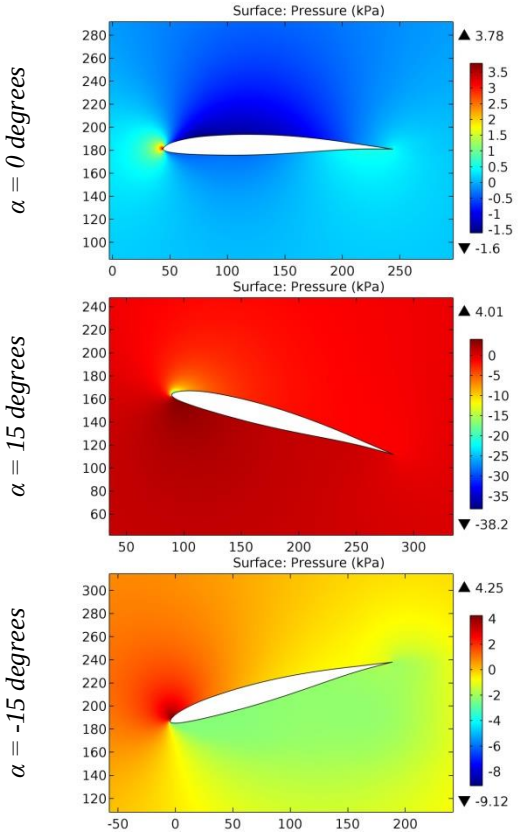

Figure 58. The pressure contours on the surfaces of the HQ 2,0-9 airfoil.

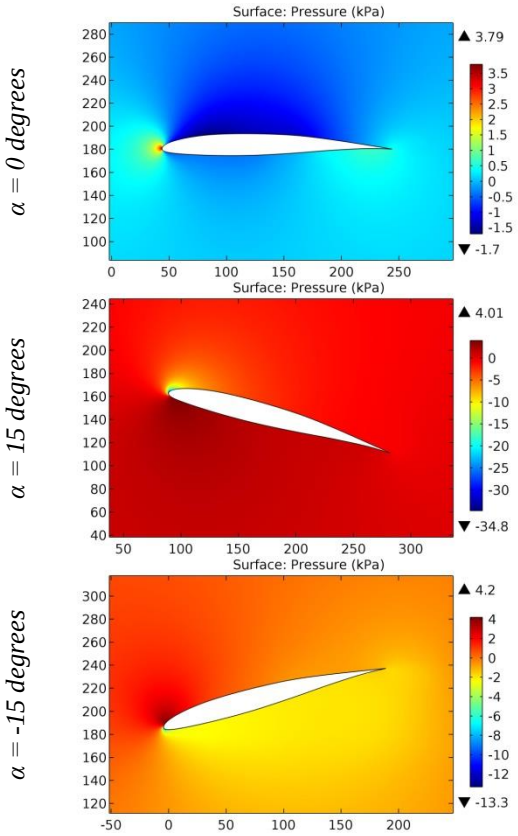

Figure 59. The pressure contours on the surfaces of the HQ 2,1-9,5 airfoil.

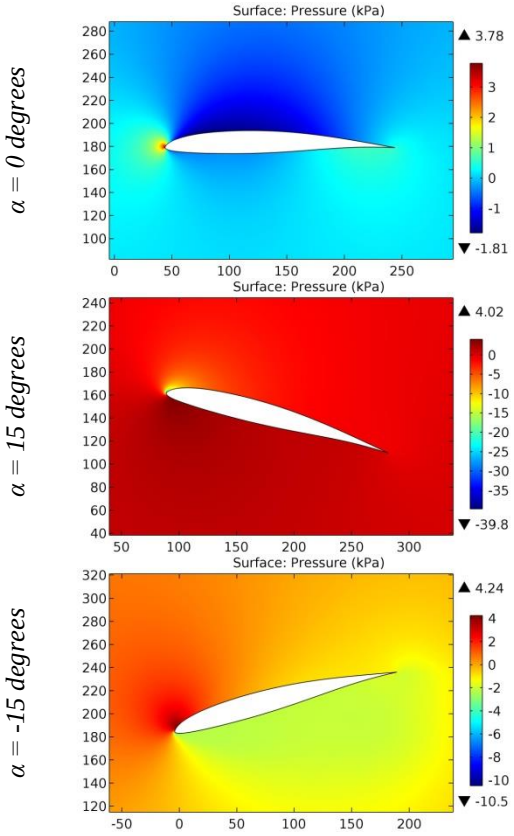

Figure 60. The pressure contours on the surfaces of the HQ 2,5-10 airfoil.

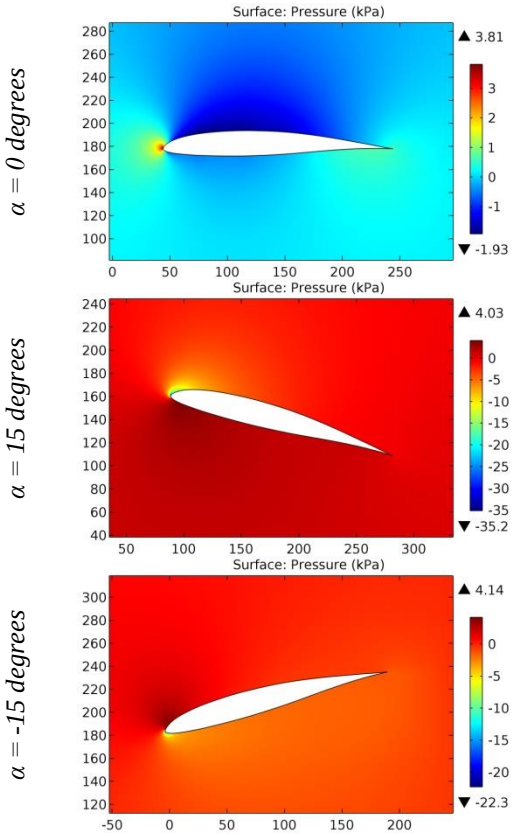

Figure 61. The pressure contours on the surfaces of the HQ 2,5-11 airfoil.

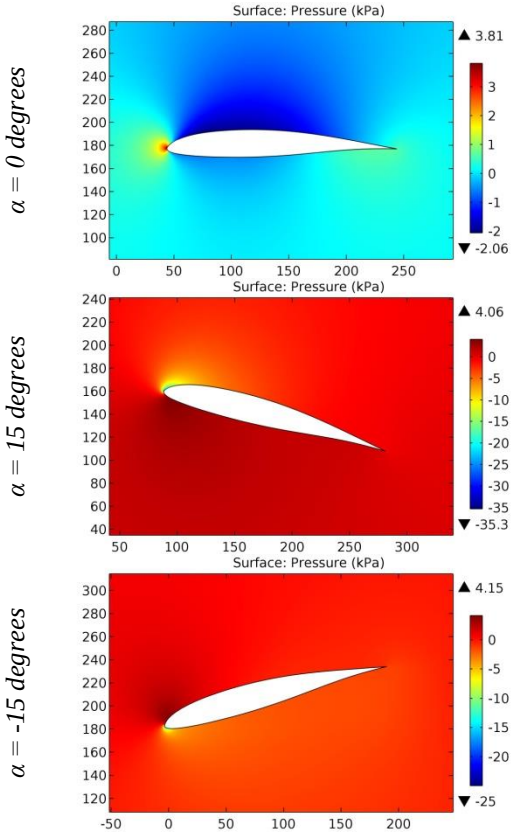

Figure 62. The pressure contours on the surfaces of the HQ 2,5-12 airfoil.

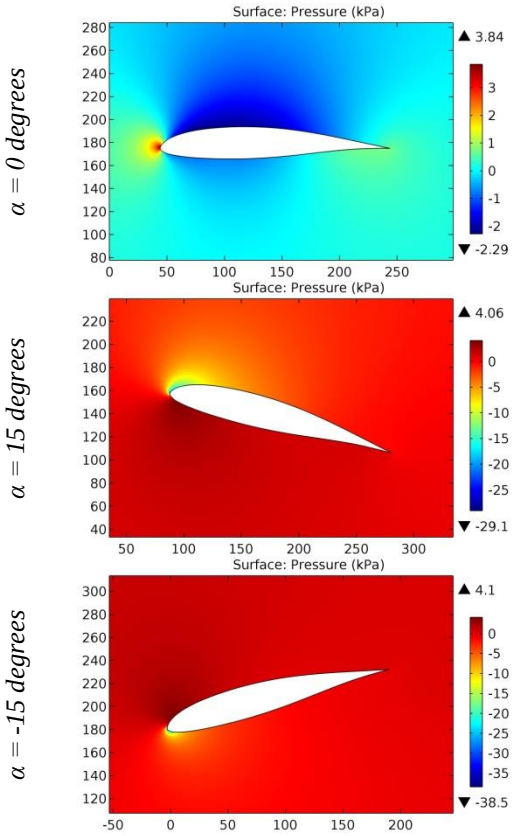

Figure 63. The pressure contours on the surfaces of the HQ 2,5-14 airfoil.

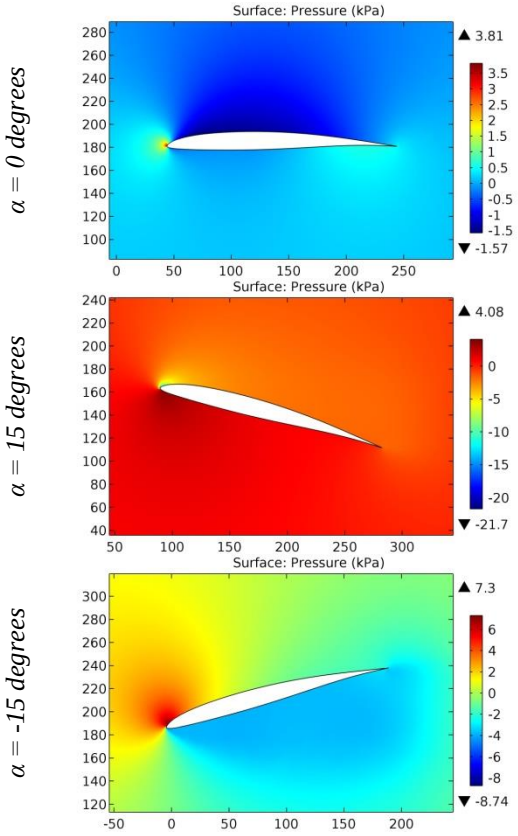

Figure 64. The pressure contours on the surfaces of the HQ 2,5-8 airfoil.

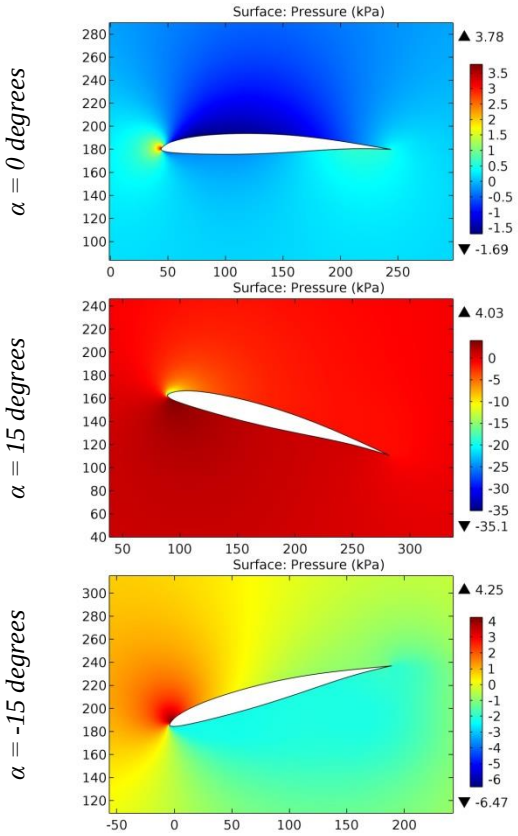

Figure 65. The pressure contours on the surfaces of the HQ 2,5-9 airfoil.

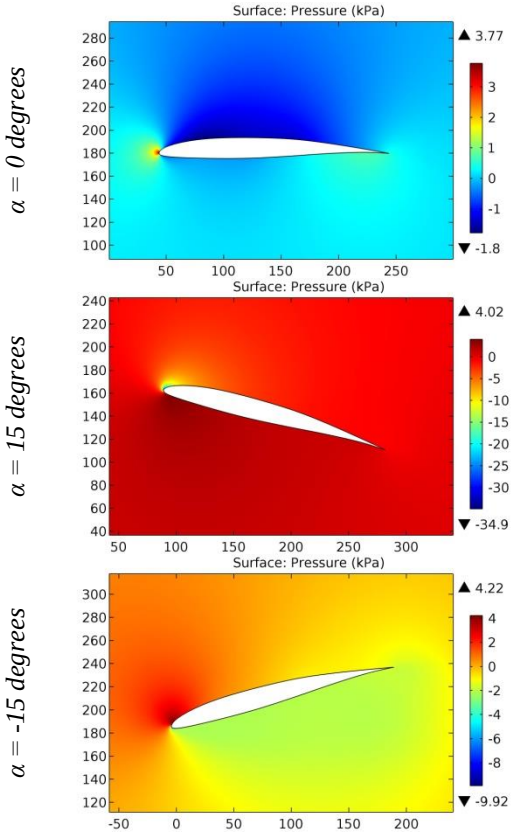

Figure 66. The pressure contours on the surfaces of the HQ 2,5-9 B airfoil.

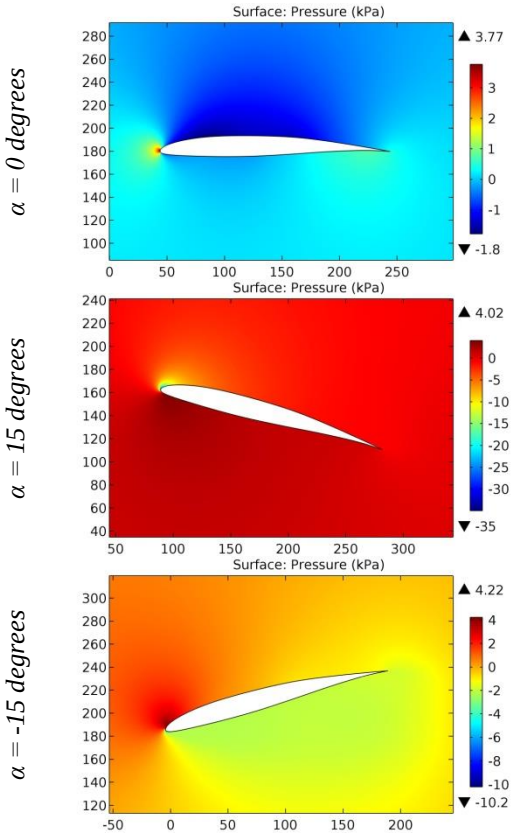

Figure 67. The pressure contours on the surfaces of the HQ 2,5-9,0 smoothed by Eppler airfoil.

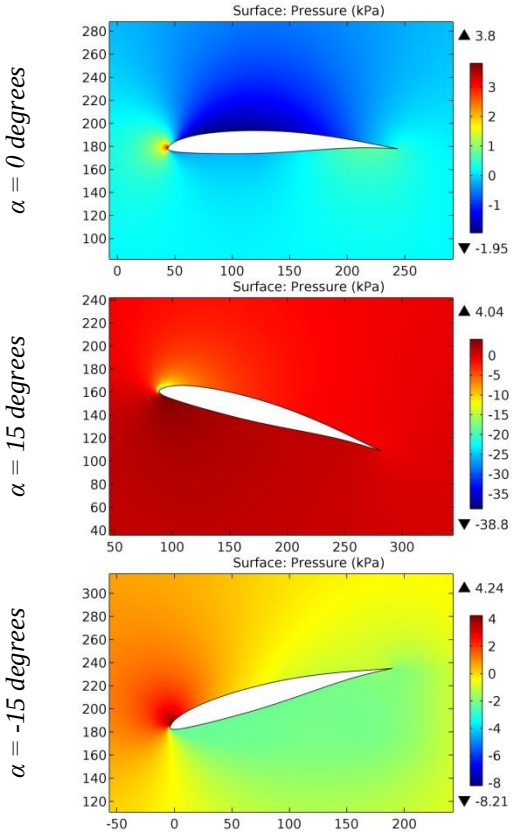

Figure 68. The pressure contours on the surfaces of the HQ 3,0-10 airfoil.

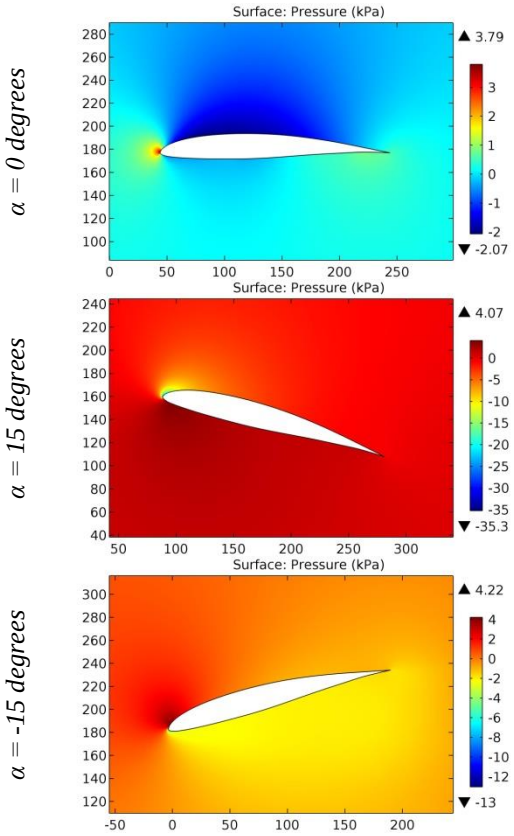

Figure 69. The pressure contours on the surfaces of the HQ 3,0-11 airfoil.

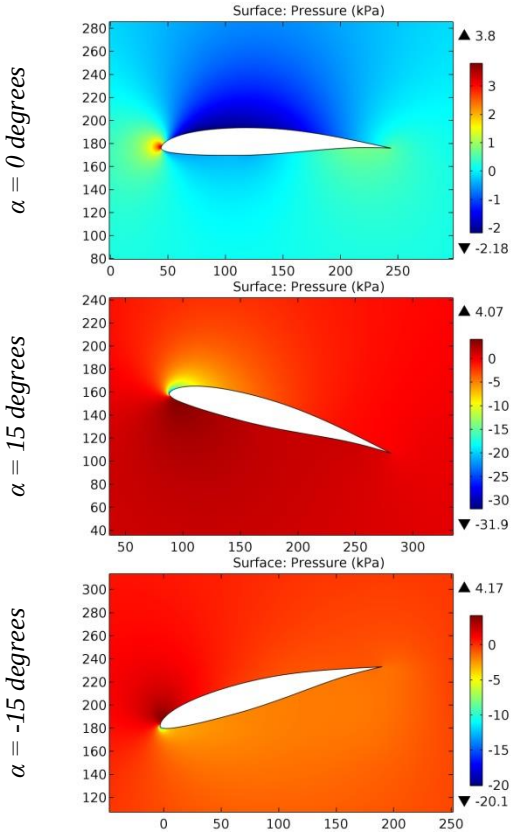

Figure 70. The pressure contours on the surfaces of the HQ 3,0-12 airfoil.

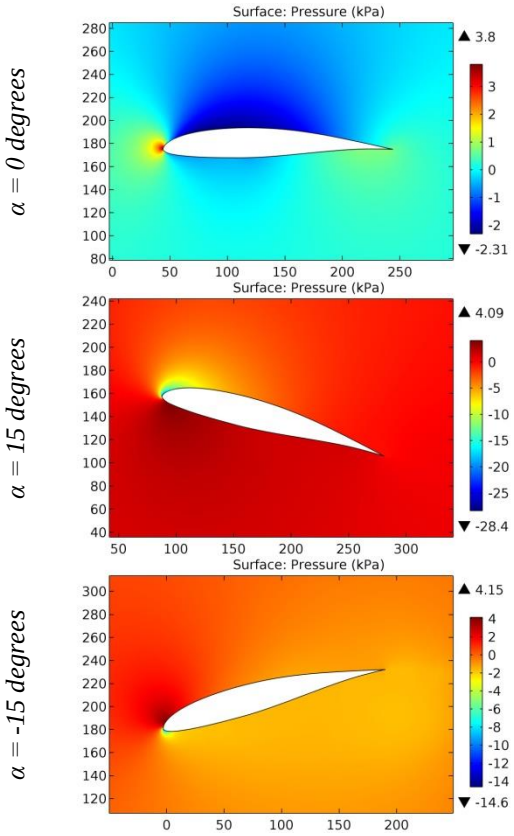

Figure 71. The pressure contours on the surfaces of the HQ 3,0-13 airfoil.

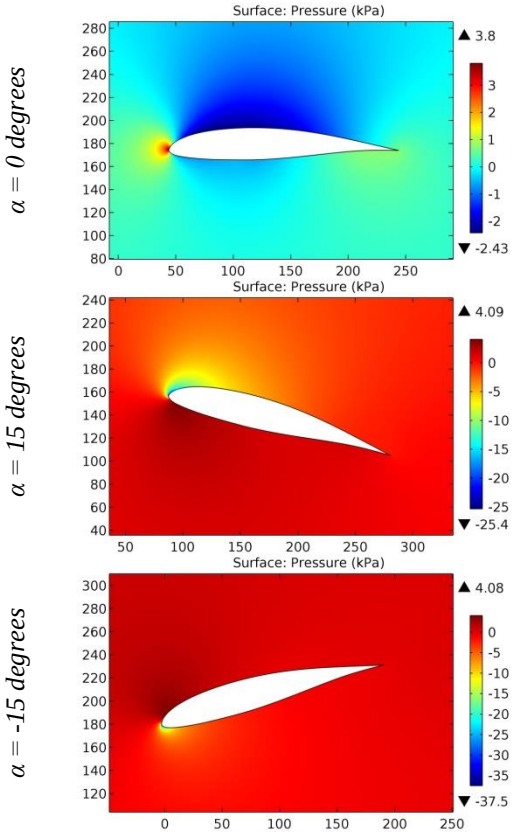

Figure 72. The pressure contours on the surfaces of the HQ 3,0-14 airfoil.

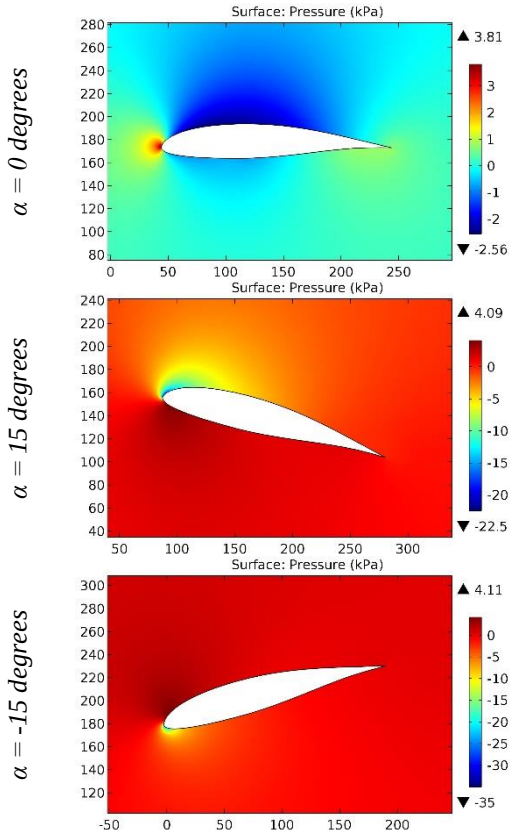

Figure 73. The pressure contours on the surfaces of the HQ 3,0-15 airfoil.

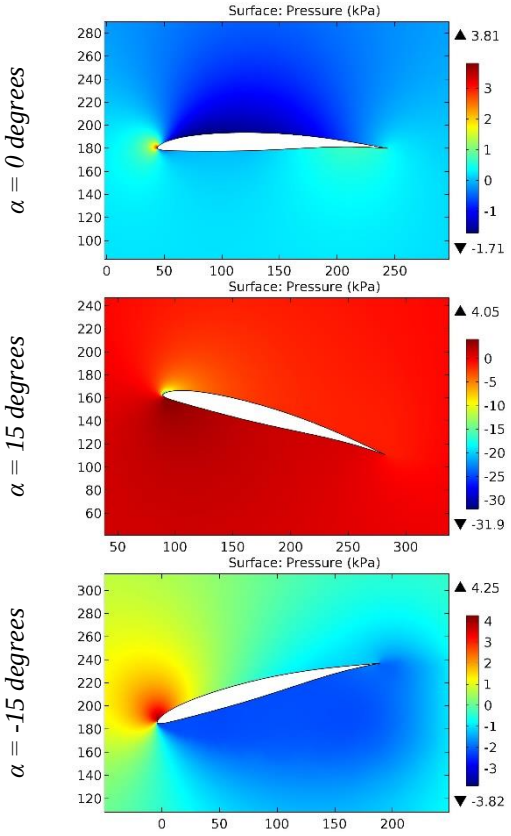

Figure 74. The pressure contours on the surfaces of the HQ 3,0-8 airfoil.

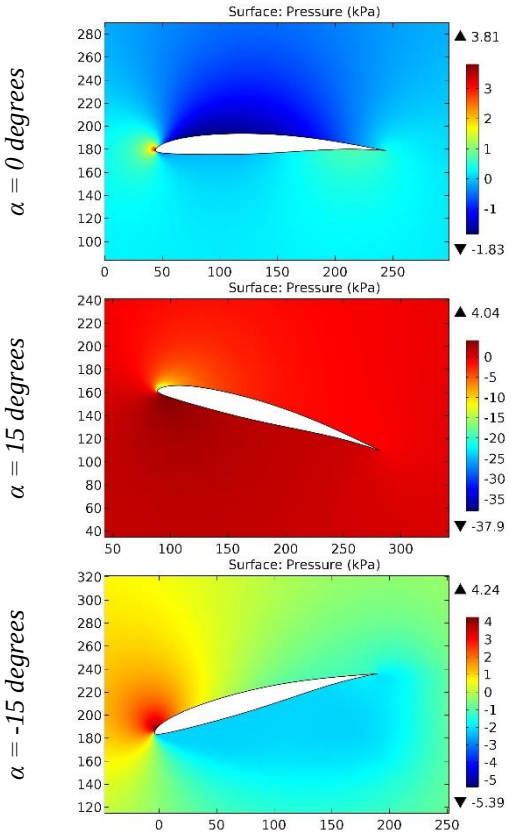

Figure 75. The pressure contours on the surfaces of the HQ 3,0-9 airfoil.

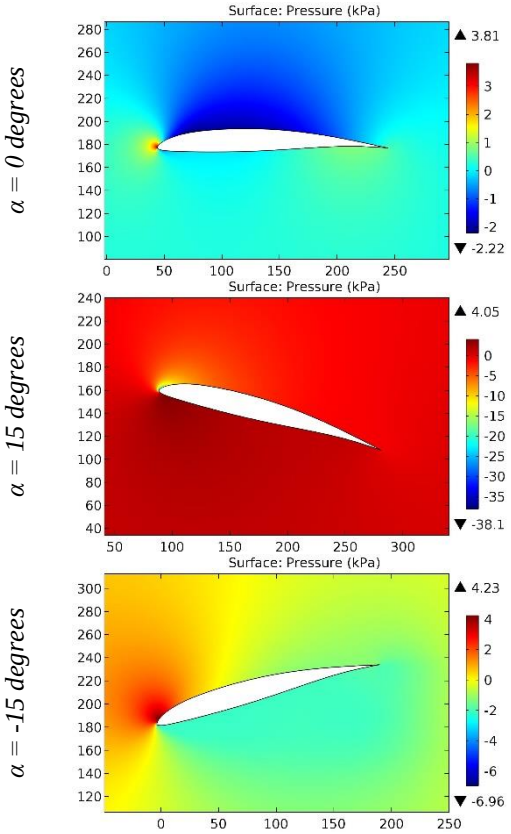

Figure 76. The pressure contours on the surfaces of the HQ 3,5-10 airfoil.

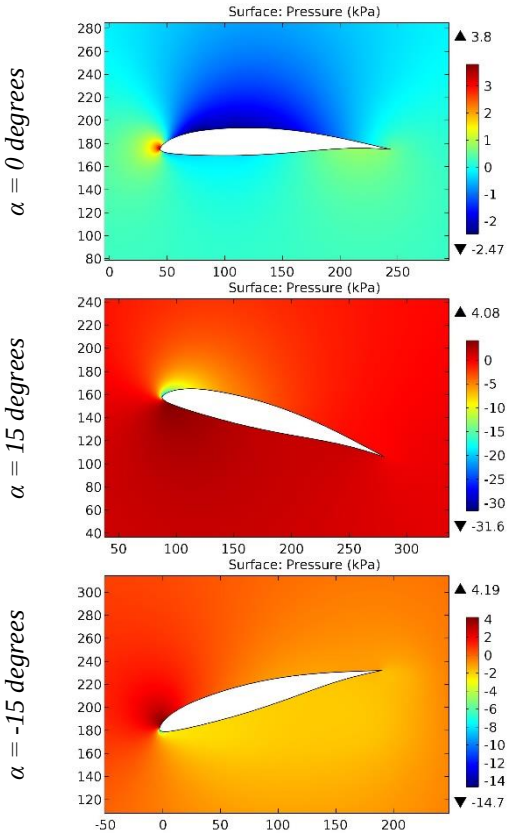

Figure 77. The pressure contours on the surfaces of the HQ 3,5-12 airfoil.

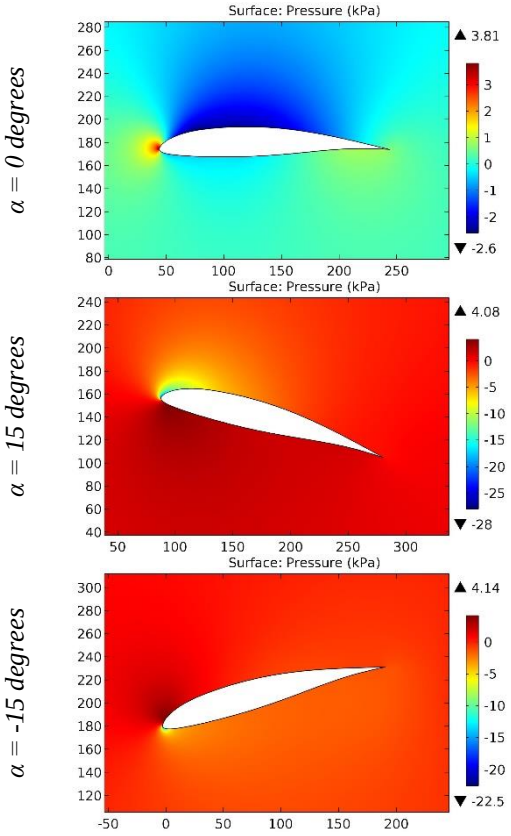

Figure 78. The pressure contours on the surfaces of the HQ 3,5-13 airfoil.

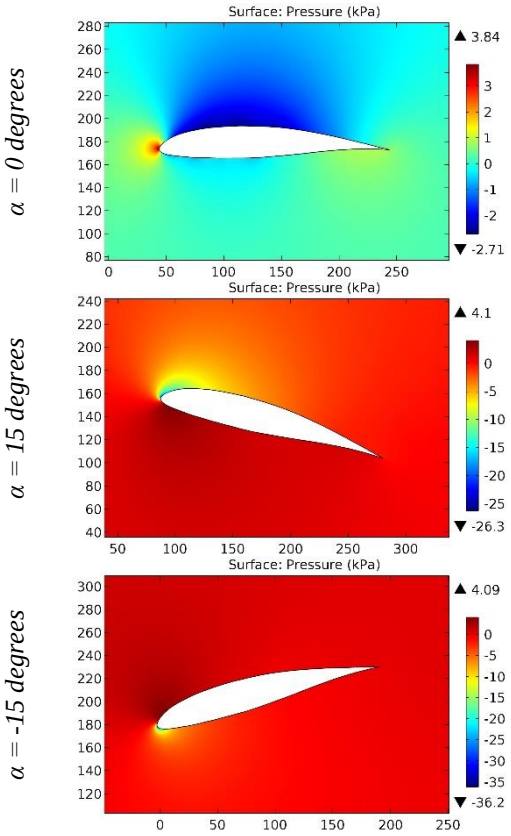

Figure 79. The pressure contours on the surfaces of the HQ 3,5-14 airfoil.

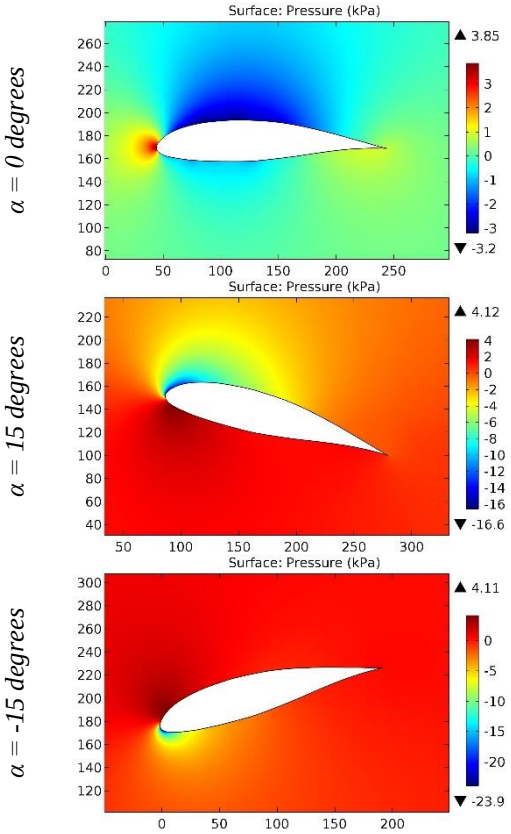

Figure 80. The pressure contours on the surfaces of the HQ 3,5-18 airfoil.

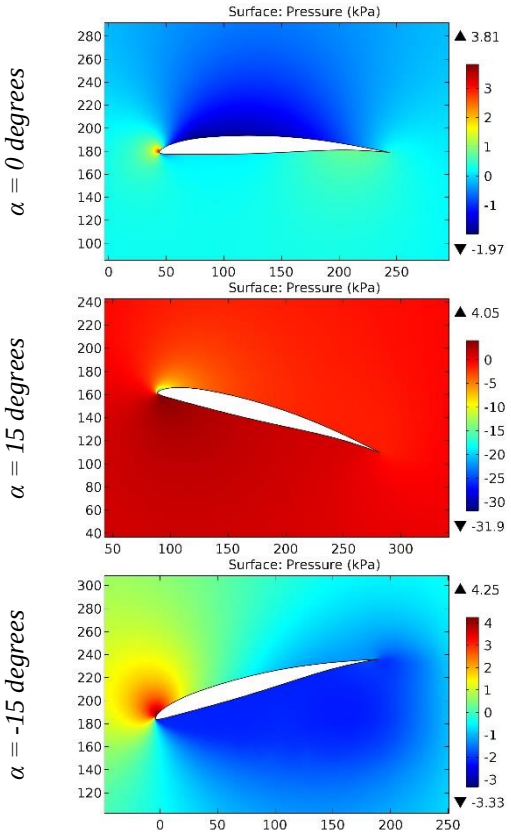

Figure 81. The pressure contours on the surfaces of the HQ 3,5-8 airfoil.

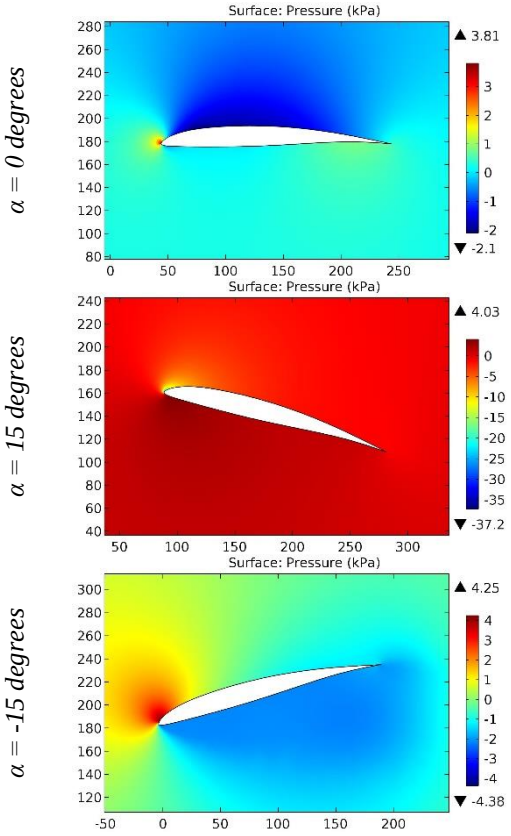

Figure 82. The pressure contours on the surfaces of the HQ 3,5-9 airfoil.

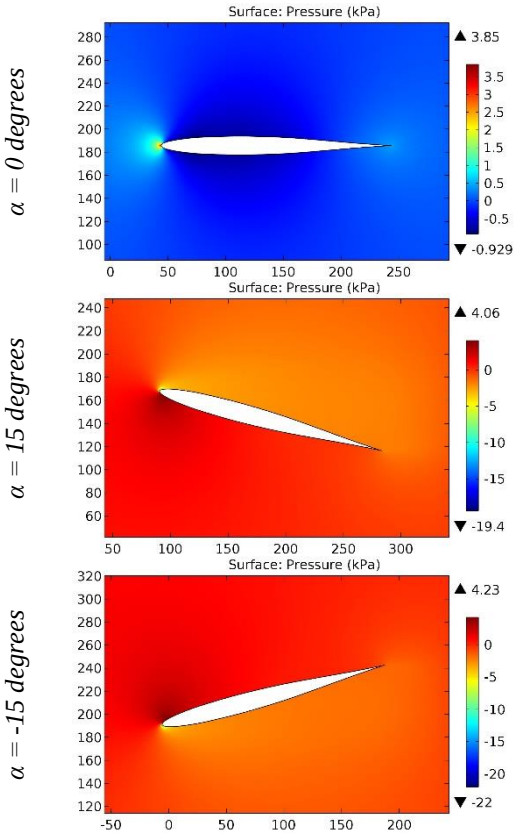

Figure 83. The pressure contours on the surfaces of the HQ-00-09 airfoil.

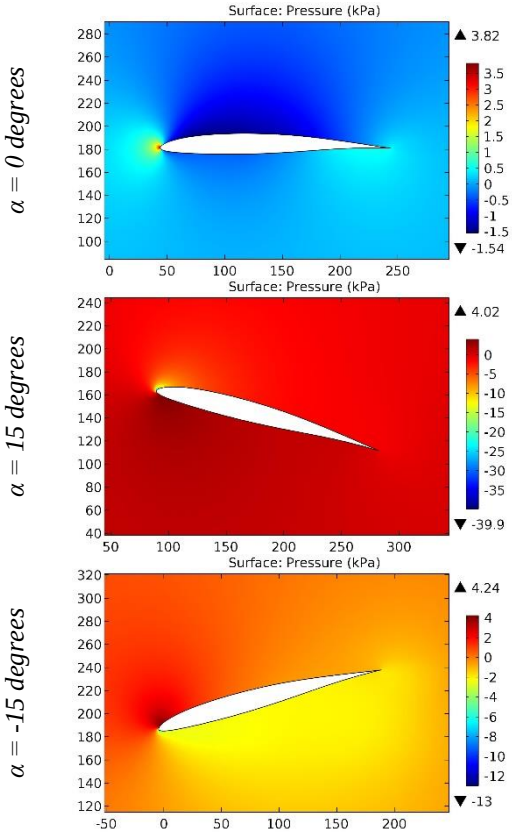

Figure 84. The pressure contours on the surfaces of the HQ-2,0-9 9,0% smoothed airfoil.

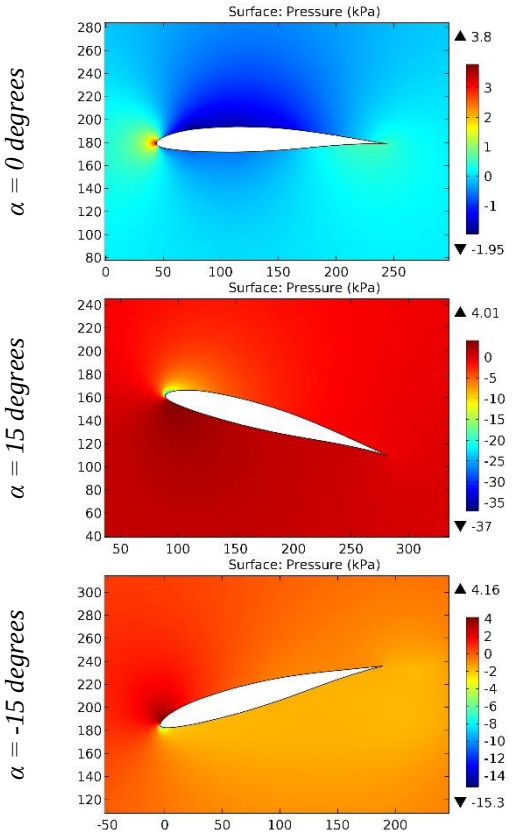

Figure 85. The pressure contours on the surfaces of the HQ-20-11 airfoil.

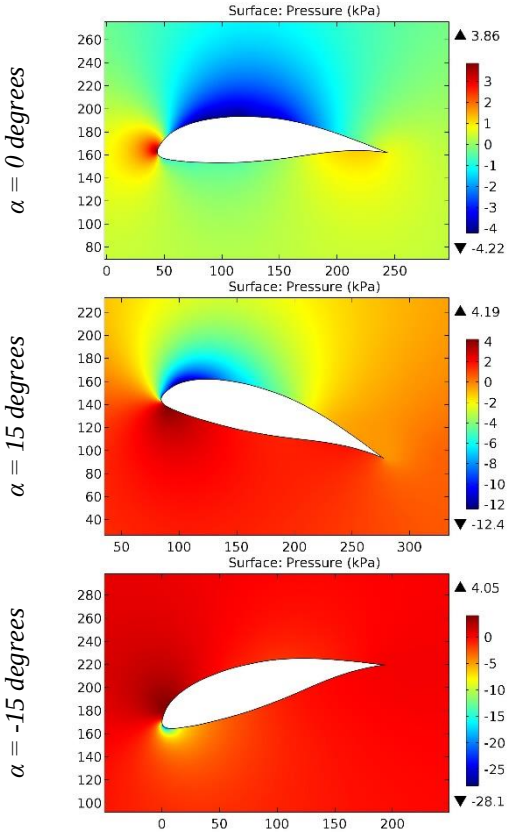

Figure 86. The pressure contours on the surfaces of the HQ-60-20 airfoil.

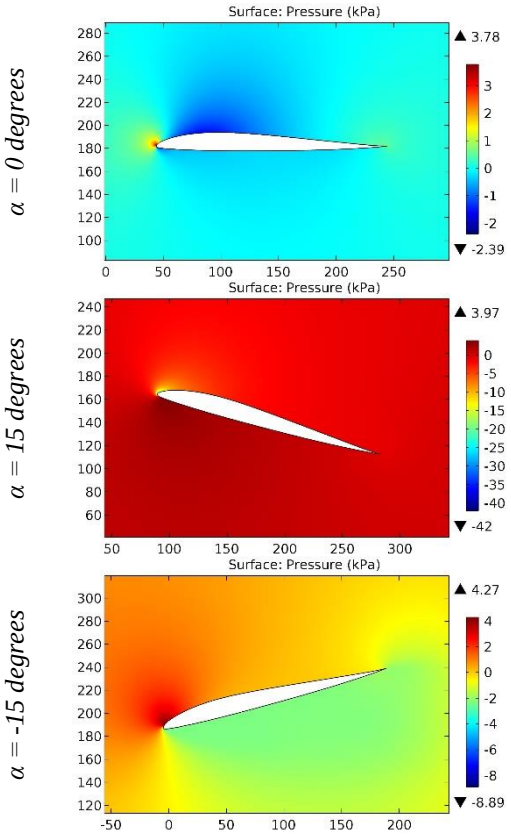

Figure 87. The pressure contours on the surfaces of the HS 2.0/8.0 airfoil.

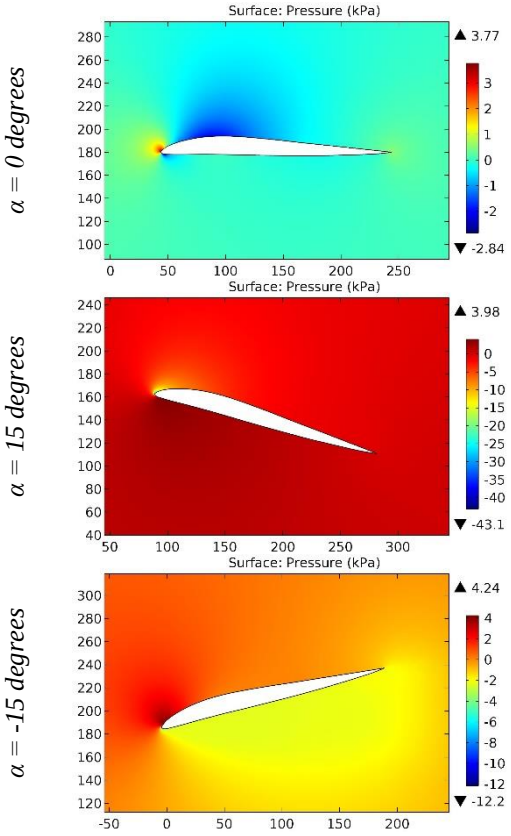

Figure 88. The pressure contours on the surfaces of the HS 3.0/8 airfoil.

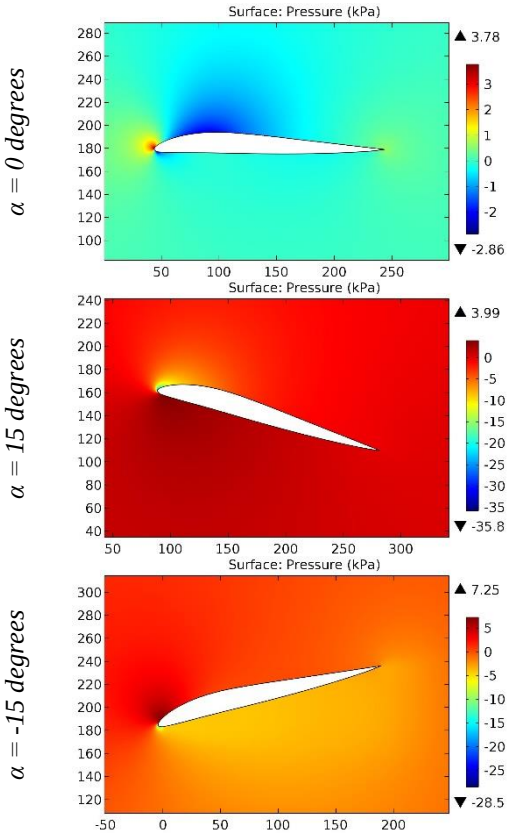

Figure 89. The pressure contours on the surfaces of the HS 3.0/9.0 airfoil.

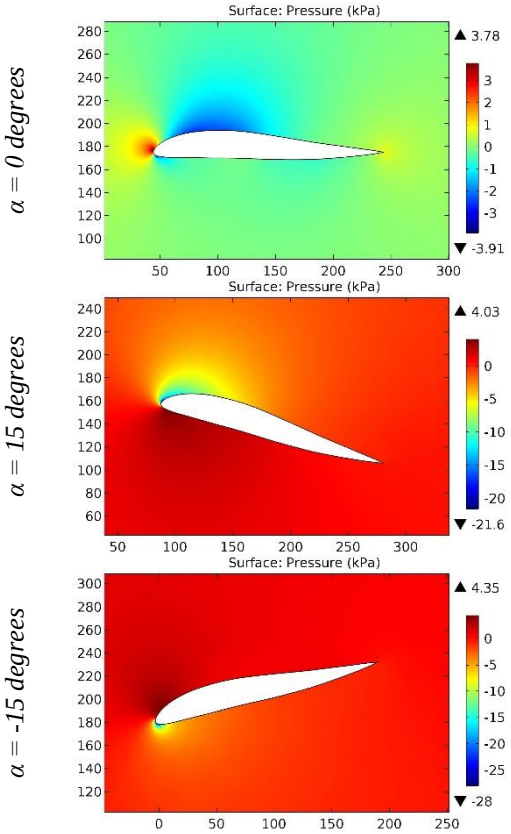

Figure 90. The pressure contours on the surfaces of the HS 3.5/12 airfoil.

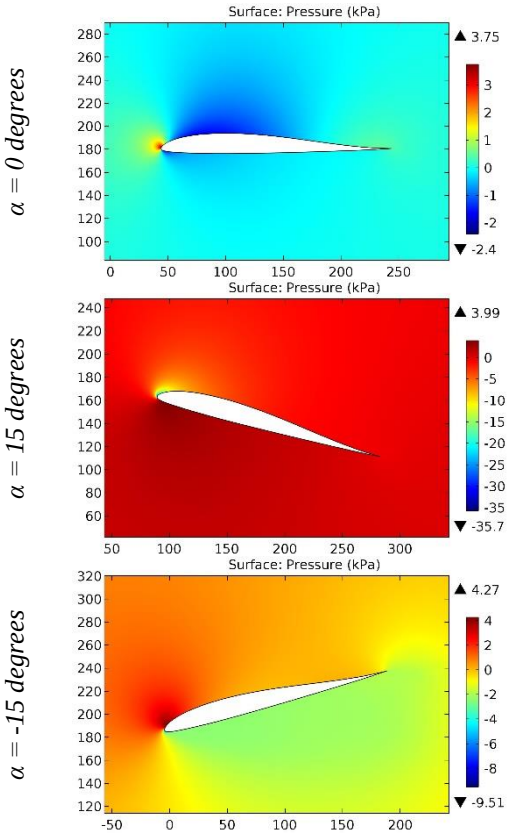

Figure 91. The pressure contours on the surfaces of the HS 510 airfoil.

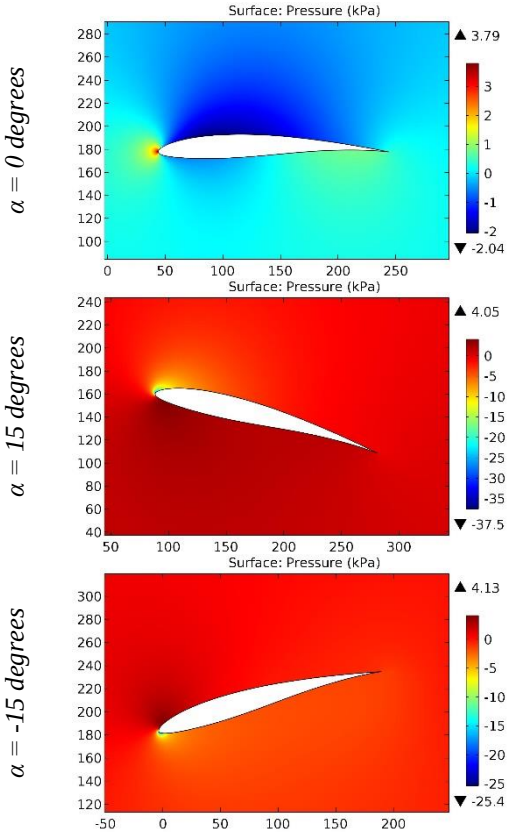

Figure 92. The pressure contours on the surfaces of the HS 602 airfoil.

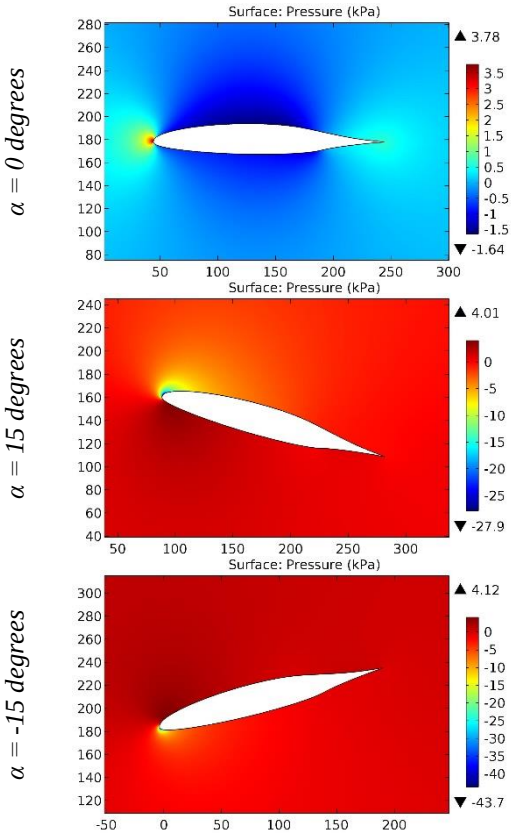

Figure 93. The pressure contours on the surfaces of the HSNLF(1)-0213 airfoil.

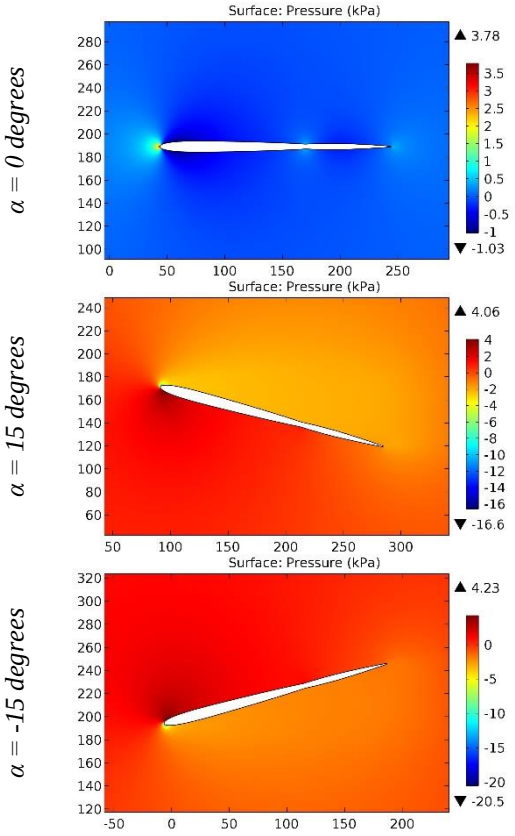

Figure 94. The pressure contours on the surfaces of the HT 05 airfoil.

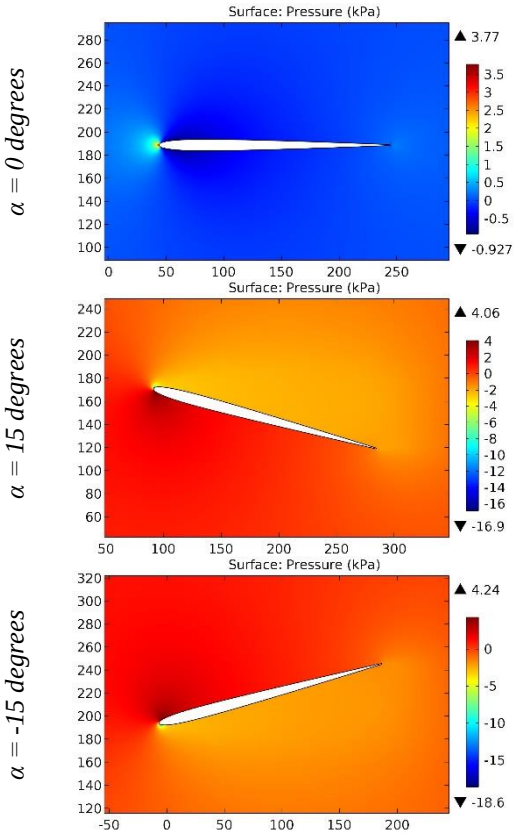

Figure 95. The pressure contours on the surfaces of the HT 08 airfoil.

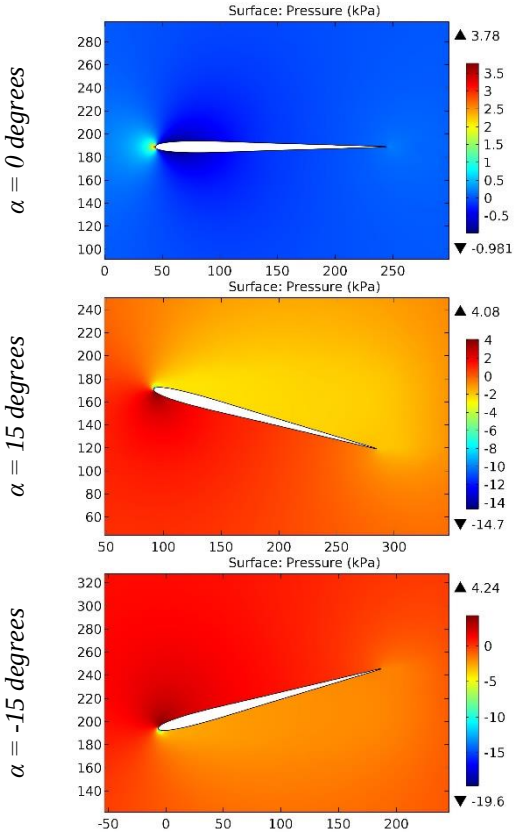

Figure 96. The pressure contours on the surfaces of the HT 12 airfoil.

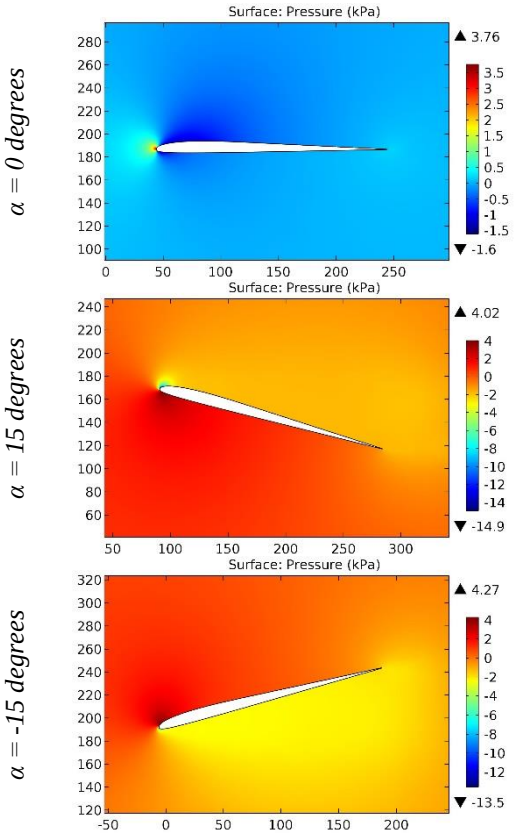

Figure 97. The pressure contours on the surfaces of the HT22 airfoil.

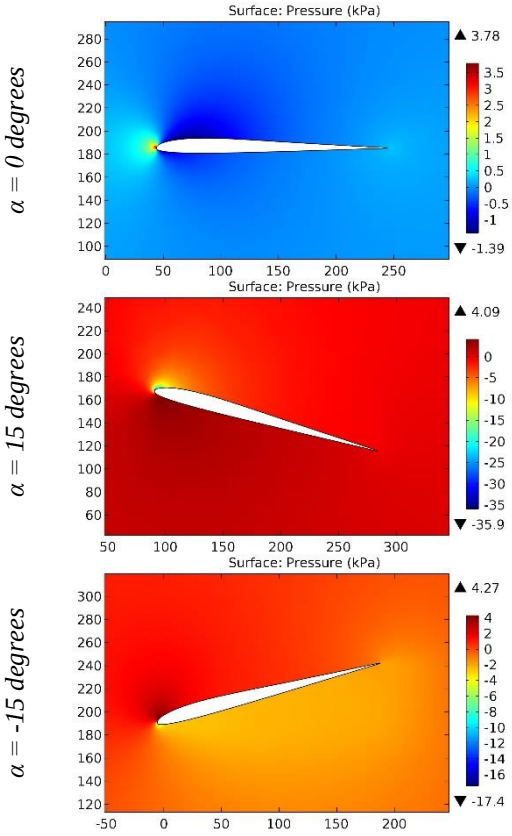

Figure 98. The pressure contours on the surfaces of the HT23 airfoil.

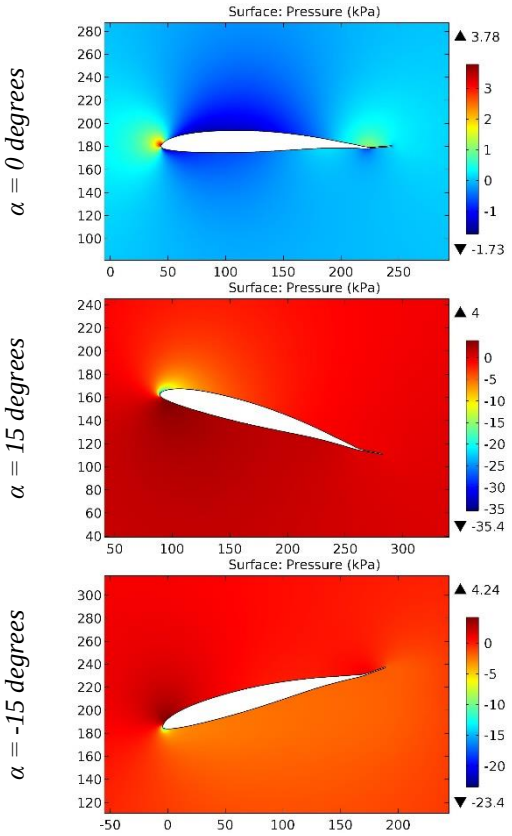

Figure 99. The pressure contours on the surfaces of the HUGHES HELICOPTERS HH-02 airfoil.

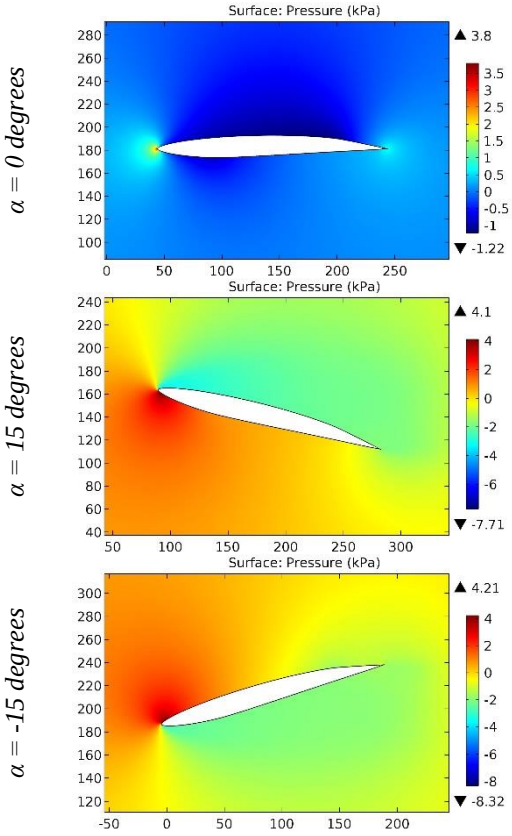

Figure 100. The pressure contours on the surfaces of the hydrofoil"Profile 915".

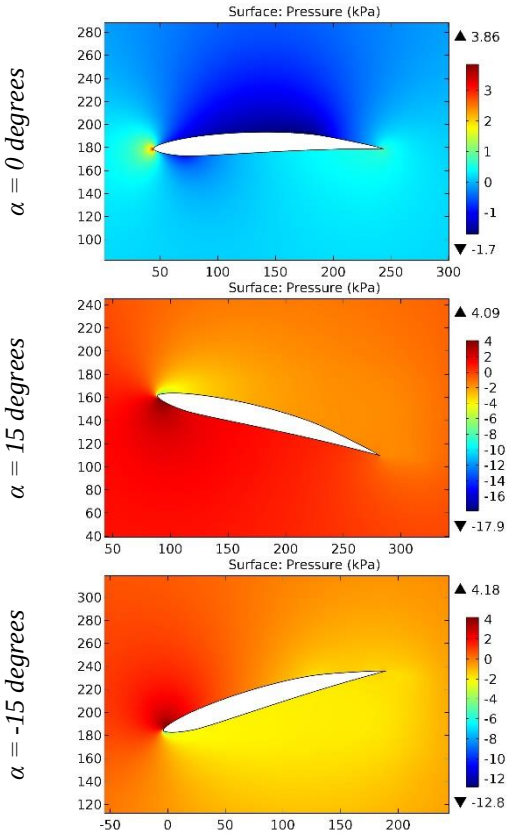

Figure 101. The pressure contours on the surfaces of the hydrofoil"Profile 930".

The values of the drag on the leading edge of the airfoils of asymmetrical geometric shapes were determined. The highest drag coefficient was calculated for the HN-956 airfoil among them. The value was calculated at the angle of attack of 0 degrees. The HO1U airfoil has the lowest drag coefficient during horizontal flight of the airplane. Thus, the decrease in the drag coefficient for the considered asymmetrical airfoils is about 25%. Similarly, the drag coefficient reduction of 2.5% was determined among the symmetrical airfoils with the maximum drag (HQ 0-7, pressure was 3.87 kPa) and the minimum drag (HN-976S, HT 05 and HT 12, pressure was 3.78 kPa).

Analyzing the simulation data, it was noted that for the HO1U airfoil, the value of the drag coefficient practically does not change during the descent and the climb of the airplane and is the minimum of all the airfoils considered above.

The maximum difference in the drag coefficient during the airplane maneuvers is observed for the HSNLF(1)-0213 airfoil. The drag increases by 1.56 times during the descent of the airplane.

Let us consider the HORSTMANN AND QUAST HQ-300 GD(MOD 2) and HUGHES HELICOPTERS HH-02 airfoils during horizontal flight of the airplane and the helicopter. These airfoils have a clockwise and counterclockwise curvature of the trailing edge. In the area of the curvature, positive air flow pressure of the greater value is formed than on the rest of the contour of the airfoil. The pressure difference is not observed during the airplane maneuvers.

Conclusion

The analysis of the calculation results showed that the change in the drag coefficient for the considered asymmetrical and symmetrical airfoils differs by the factor of 10. The significant part of the airfoils and hydrofoils during the climb of the airplane has the large lifting force, which is confirmed by the large difference in positive and negative pressures on the upper and lower surfaces.

References:

1. Anderson, J. D. (2010). *Fundamentals of Aerodynamics*. McGraw-Hill, Fifth edition.
2. Shevell, R. S. (1989). *Fundamentals of Flight.* Prentice Hall, Second edition.
3. Houghton, E. L., & Carpenter, P. W. (2003). *Aerodynamics for Engineering Students*. Fifth edition, Elsevier.
4. Lan, E. C. T., & Roskam, J. (2003). *Airplane Aerodynamics and Performance.* DAR Corp.
5. Sadraey, M. (2009). *Aircraft Performance Analysis.* VDM Verlag Dr. Müller.
6. Anderson, J. D. (1999). *Aircraft Performance and Design.* McGraw-Hill.
7. Roskam, J. (2007). *Airplane Flight Dynamics and Automatic Flight Control*, Part I. DAR Corp.
8. Etkin, B., & Reid, L. D. (1996). *Dynamics of Flight, Stability and Control.* Third Edition, Wiley.
9. Stevens, B. L., & Lewis, F. L. (2003). *Aircraft Control and Simulation.* Second Edition, Wiley.
10. Chemezov, D., et al. (2021). Pressure distribution on the surfaces of the NACA 0012 airfoil under conditions of changing the angle of attack. *ISJ Theoretical & Applied Science, 09 (101)*, 601-606.
11. Chemezov, D., et al. (2021). Stressed state of surfaces of the NACA 0012 airfoil at high angles of attack. *ISJ Theoretical & Applied Science, 10 (102)*, 601-604.
12. Chemezov, D., et al. (2021). Reference data of pressure distribution on the surfaces of airfoils having the names beginning with the letter A (the first part). *ISJ Theoretical & Applied Science, 10 (102)*, 943-958.
13. Chemezov, D., et al. (2021). Reference data of pressure distribution on the surfaces of airfoils having the names beginning with the letter A (the second part). *ISJ Theoretical & Applied Science, 11 (103)*, 656-675.
14. Chemezov, D., et al. (2021). Reference data of pressure distribution on the surfaces of airfoils having the names beginning with the letter B. *ISJ Theoretical & Applied Science, 11 (103)*, 1001-1076.
15. Chemezov, D., et al. (2021). Reference data of pressure distribution on the surfaces of airfoils having the names beginning with the letter C. *ISJ Theoretical & Applied Science, 12 (104)*, 814-844.
16. Chemezov, D., et al. (2021). Reference data of pressure distribution on the surfaces of airfoils having the names beginning with the letter D. *ISJ Theoretical & Applied Science, 12 (104)*, 1244-1274.
17. Chemezov, D., et al. (2022). Reference data of pressure distribution on the surfaces of airfoils (hydrofoils) having the names beginning with

the letter E (the first part). *ISJ Theoretical & Applied Science, 01 (105)*, 501-569.

18. Chemezov, D., et al. (2022). Reference data of pressure distribution on the surfaces of airfoils (hydrofoils) having the names beginning with the letter E (the second part). *ISJ Theoretical & Applied Science, 01 (105)*, 601-671.
19. Chemezov, D., et al. (2022). Reference data of pressure distribution on the surfaces of airfoils having the names beginning with the letter F. *ISJ Theoretical & Applied Science, 02 (106)*, 101-135.
20. Chemezov, D., et al. (2022). Reference data of pressure distribution on the surfaces of airfoils having the names beginning with the letter G (the first part). *ISJ Theoretical & Applied Science, 03 (107)*, 701-784.
21. Chemezov, D., et al. (2022). Reference data of pressure distribution on the surfaces of airfoils having the names beginning with the letter G (the second part). *ISJ Theoretical & Applied Science, 03 (107)*, 901-984.
22. Chemezov, D., et al. (2022). Reference data of pressure distribution on the surfaces of airfoils having the names beginning with the letter G (the third part). *ISJ Theoretical & Applied Science, 04 (108)*, 401-484.